

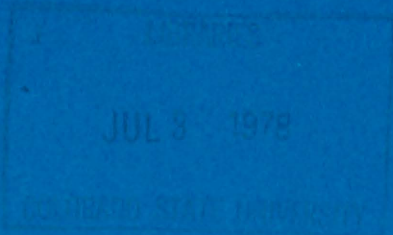
QC852
C6
no. 280
ARCHIVE

CHARACTERISTIC SIZE SPECTRA OF CUMULUS FIELDS OBSERVED FROM SATELLITES

MALCOLM D. GIFFORD
THOMAS B. McKEE



Atmospheric Science
PAPER NO.
280



US ISSN 0067-0340

DEPARTMENT OF ATMOSPHERIC SCIENCE
COLORADO STATE UNIVERSITY
FORT COLLINS, COLORADO

CHARACTERISTIC SIZE SPECTRA OF CUMULUS FIELDS
OBSERVED FROM SATELLITES

By

Malcolm Douglas Gifford
Thomas B. McKee

The research reported here has been supported
by the United States Air Force
and National Science Foundation
Grants OCD 75-13924 and ATM 76-80568.

Department of Atmospheric Science
Colorado State University
Fort Collins, Colorado

November 1977

Atmospheric Science Paper No. 280

ABSTRACT

A technique is presented which allows the investigator to monitor size distributions of small scale cumulus fields using satellite data. The limitations of the technique are shown to be the resolution and quality of the satellite imagery.

Twenty-four samples of small cumulus are studied using DMSP and SMS-1 satellite imagery. A total of eleven DMSP samples are examined from North Carolina and Florida. These samples are compared to six DMSP samples and seven SMS-1 samples drawn from cumulus fields observed over the subtropical and tropical Atlantic Ocean. Comparisons are based on parameters derived from the least-squares solutions of a linearized first order exponential model.

An exponential decrease in cloud number density with increasing cloud diameter is exhibited in both the mean cloud number density distributions of the case studies and the cloud number density distributions of selected typical cumulus samples. The poorer data quality of the SMS-1 imagery is seen to cause deviations from the exponential model in approximately 40% of the samples.

The coefficient of exponential decrease in cloud number density is shown to lie in the interval 0.59 to 1.51 km^{-1} . These values are seen to be in excellent agreement with the results of previous investigators.

A comparison is made between typical samples of oceanic and continental cloud number density distributions. Although a significant increase in regression slope is seen in the oceanic sample, further research is suggested to bolster current evidence.

ACKNOWLEDGEMENTS

The authors wish to express thanks to Ms. Janella Owen Ashbaugh for drafting the figures, Ms. Gayle Meltesen for her suggestions concerning the statistical analysis of the data, and to Ms. Dorothy Chapman for her assistance in typing the manuscript.

This research effort was made possible through the combined resources of the United States Air Force and National Science Foundation grant numbers OCD 75-13924 and ATM 76-80568.

TABLE OF CONTENTS

	<u>Page</u>
ABSTRACT.....	ii
ACKNOWLEDGEMENTS.....	iii
TABLE OF CONTENTS.....	iv
LIST OF FIGURES.....	vi
LIST OF TABLES.....	vii
1.0 INTRODUCTION.....	1
1.1 Purpose.....	1
1.2 Previous Research.....	3
1.3 Distribution Equations.....	5
1.4 Satellite Applicability.....	9
2.0 SAMPLING PROCEDURE.....	11
2.1 Selection of Data.....	11
2.2 Data Processing.....	11
2.3 Equipment.....	13
2.4 Automated Sampling.....	14
3.0 CASE STUDIES.....	16
3.1 Data Sets.....	16
3.1.1 North Carolina.....	17
3.1.2 Florida.....	24
3.1.3 DMSP Oceanic.....	29
3.1.4 SMS-1 Oceanic.....	29
3.2 Discussion.....	42
3.2.1 Comparison of Case Studies.....	42
3.2.2 Group Structure Analysis.....	48

TABLE OF CONTENTS Continued

	<u>Page</u>
3.2.3 Statistical Analysis.....	52
3.2.4 Comparison to Previous Research.....	55
4.0 CONCLUSIONS.....	64
REFERENCES.....	67
APPENDIX A. STATISTICAL RESULTS.....	68
APPENDIX B. SELECTION OF TYPICAL SAMPLES.....	75
APPENDIX C. COMPARISON OF REGRESSION SLOPES.....	78

LIST OF FIGURES

<u>Figure</u>		<u>Page</u>
1	Location of DMSP Case Studies.....	18
2	North Carolina Case Study.....	21
3	Observed Mean Sky Cover Contributions, North Carolina Case Study.....	23
4	Florida Case Study.....	26
5	Observed Mean Sky Cover Contributions, Florida Case Study.....	28
6	DMSP Oceanic Case Study.....	32
7	Observed Mean Sky Cover Contributions, DMSP Oceanic Case Study.....	34
8	Locations of SMS-1 Sampling Areas.....	36
9	SMS-1 Oceanic Case Study.....	39
10	Observed Mean Sky Cover Contributions, SMS-1 Oceanic Case Study.....	41
11	Configurations of Clouds Observed in Sampling.....	49
12	Typical North Carolina Sample, 2 June 1973.....	56
13	Typical Florida Sample, 14 June 1973.....	57
14	Typical DMSP Oceanic Sample, 29 August 1973.....	58
15	Typical SMS-1 Oceanic Sample, Day 247, 1974.....	59

LIST OF TABLES

<u>Table</u>		<u>Page</u>
1	North Carolina Case Study.....	17
2	Normalized Cloud Number Density, North Carolina Samples.....	20
3	Contributions to Total Sky Cover, North Carolina Samples.....	22
4	Florida Case Study.....	24
5	Normalized Cloud Number Density, Florida Samples.....	25
6	Contributions to Total Sky Cover, Florida Samples.....	27
7	DMSP Oceanic Case Study.....	30
8	Normalized Cloud Number Density, DMSP Oceanic Samples.....	31
9	Contributions to Total Sky Cover, DMSP Oceanic Samples.....	33
10	SMS-1 Oceanic Case Study.....	37
11	Normalized Cloud Number Density, SMS-1 Oceanic Samples.....	38
12	Contributions to Total Sky Cover, SMS-1 Oceanic Samples.....	40
13	Summary of Case Study Parameters.....	43
14	Summary of Results, Cloud Groups Excluded.....	51
15	Summary of Parameters for Typical Cumulus Samples.....	60
1A	AOV Table for North Carolina Case Study. Cloud group structures are included in the number density distribution.....	70
2A	AOV Table for North Carolina Case Study. Cloud group structures have been eliminated from the number density distribution.....	70

LIST OF TABLES Continued

<u>Table</u>	<u>Page</u>
3A	71
AOV Table for Florida Case Study. Cloud group structures are included in the number density distribution.....	
4A	71
AOV Table for Florida Case Study. Cloud group structures have been eliminated from the number density distribution.....	
5A	72
AOV Table for SMS-1 Oceanic Case Study. Cloud group structures are included in the number density distribution.....	
6A	72
AOV Table for SMS-1 Oceanic Case Study. Cloud group structures have been eliminated from the number density distribution.....	
7A	73
AOV Table for DMSP Oceanic Case Study. Cloud group structures are included in the number density distribution.....	
8A	73
AOV Table for DMSP Oceanic Case Study. Cloud group structures have been eliminated from the number density distribution.....	
9A	74
AOV Table for DMSP Oceanic Case Study. Cloud group structures are included in the number density distribution, but the outlier (4.12 nm class) has been removed from the analysis.....	
1B	75
Normalized Cloud Number Densities for North Carolina, Excluding Cloud Groups.....	
2B	76
Normalized Cloud Number Densities for Florida, Excluding Cloud Groups.....	
3B	76
Normalized Cloud Number Densities for DMSP Oceanic Data, Excluding Cloud Groups.....	
4B	77
Normalized Cloud Number Densities for SMS-1 Oceanic Data, Excluding Cloud Groups.....	
1C	78
Comparison of Regression Slopes.....	

1.0 INTRODUCTION

1.1 Purpose

The role of the small cumulus cloud in atmospheric processes is not yet fully understood. Clouds with diameters less than 4 nm (7.4 km) or so will not produce any significant precipitation, nor are any severe weather phenomena associated with them. Then why should these seemingly insignificant clouds be the topic of research if they have so little direct effect on man?

One answer lies in the role these small clouds play in assisting larger clouds in the production of precipitation. In a study of tropical disturbances in the Atlantic, Lopez (1976) reports that 60% of the clouds associated with these disturbances never attain an area greater than 9 nm^2 (31 km^2). Yet these smaller clouds assist in the maintenance of larger precipitating clouds. Gray (1973) estimates that 20% of the area in the tropics is made up of organized cloud clusters which provide the bulk of the precipitation which falls in this region of the globe. Since the amount of precipitation in these clusters far outweighs the amount of evaporation occurring in the immediate vicinity of the cluster, water vapor must be transported into the region in order to satisfy the water vapor budget of the cluster. Gray shows that 50% of the required water vapor transport occurs in the boundary layer, while the remaining 50% must be imported in the layers between 950 mb and approximately 400 mb. The water vapor transported in these layers is that which has been processed through the smaller clouds. The added moisture in the lower and

middle troposphere required to maintain a tropical cloud cluster is thus attributable to the smaller scale cumulus by the processes of evaporation and diffusion as they grow and die. The role of smaller clouds should not be misconstrued as only being important in the tropics. The massive mid-latitude storm systems benefit from the additional water vapor in the lower and middle troposphere in the same manner as the tropical cloud clusters.

Another area in which the role of the smaller cumulus cloud cannot be ignored is in the calculation of a radiation budget. McKee and Cox (1974, 1976) have presented strong evidence that shortwave radiation interacts with finite clouds in quite a different manner than it does with semi-infinite cloud surfaces. Dynamical models which consider the interaction of incoming solar radiation with fields of small cumulus would probably improve their results if the infinite cloud assumption were replaced with the finite cloud approximations offered by McKee and Cox (1976). These approximations, used in conjunction with typical cumulus size distributions, offer a more realistic approach to the problem of cumulus parameterization in modeling.

The preceding examples are just two of many important areas in the realm of atmospheric research which could benefit from a fuller knowledge of the size distributions of these small but important clouds. The goal of this paper, therefore, is to report on the distributions obtained from four case study areas. At the same time, the techniques used in this research effort provide a simple and economical method that could be used to monitor suspected changes in size distribution in space and time.

1.2 Previous Research

Most of the investigations which have examined the size distributions of small cumulus have been conducted within the past two decades.

During the 1968 Barbados Meteorological Experiment many hours of 10 cm airborne radar data were gathered. These data were subsequently analyzed and reported in the literature by Lopez (1973, 1976). The results of Lopez (1976) are based on the observation of approximately 7400 radar echoes and generally show an exponential decrease in cloud number with increasing cloud diameter. Comparisons between his results and the current satellite study are not possible due to the stratification of the radar data. The resolution of the 10 cm radar forced Lopez to use a class interval of 9 nm^2 (31 km^2), corresponding to a diameter range of zero to 3.4 nm (6.3 km) for the smallest class. In chapter three of this paper, it will be shown that the distribution curves of all typical satellite samples will easily fit within the first class interval used by Lopez.

Recent satellite cloud climatologies have been conducted by Reynolds and Vonder Haar (1975) and Stodt and Grant (1976). Both studies drew samples from the high plains area of the midwestern United States. The Reynolds and Vonder Haar samples were taken from the Applications Technology Satellite (ATS-3) which has a resolution of 6.5 nm (12 km). All of the clouds tabulated in the typical samples of the current study were found to be too small to be detectable by the ATS-3 sensor. The poor resolution of ATS-3, along with the subjective cloud classification system used in their study, make the

results of Reynolds and Vonder Haar unsuited for comparison with current results. The study by Stodt and Grant, modeled after the research done by Reynolds and Vonder Haar, used the same type of subjective cloud classification system. Even though the resolution of the data analyzed by Stodt and Grant was identical to that of the present study, the subjective classification system prevents any meaningful comparison.

A most extensive photographic study was conducted by Plank (1969), involving approximately 150,000 photographs taken by high-altitude reconnaissance aircraft over the Florida peninsula. From these photographs a set of thirty-four samples was chosen, of which nineteen were analyzed in greater detail. These nineteen samples were chosen to represent above average, average, and below average sky cover conditions. The final samples were also chosen from various observation times in order to more adequately represent the diurnal convective cycle. Photogrammetric analysis of the samples provided the following information:

1. Cloud base altitude estimates based on shadow-displacement techniques.
2. Cloud base horizontal dimensions.
3. An estimate of the height-diameter relationships.

These data were then further analyzed to determine the contributions made by each size-class to the total sky cover and total cloudy volume.

In his paper Plank also summarized the results of a similar photographic study conducted by Blackmer and Serebreny (1962). They

gathered eleven samples from cumulus populations observed during two aircraft reconnaissance flights between California and Florida. The results obtained by Blackmer and Serebreny were found to be quite similar to those reported by Plank.

Due to the similarities between high-altitude reconnaissance photographs and very high resolution satellite imagery, the satellite study summarized in this paper was patterned after the research efforts of Plank, Blackmer, and Serebreny.

1.3 Distribution Equations

In order that he might compare his results with those of Blackmer and Serebreny, Plank developed a simple exponential model to describe the size distributions which he had observed. The parameters of the model equation were then used in deriving other equations which approximate the observed sky cover distribution. The size distribution equation was also transformed into a cloud volume distribution function. Since cloud height-diameter relationships were not obtainable in the current study, the cloud volume distribution function will not be presented in this paper.

The number density distribution function expressed by Plank as

$$n = Ke^{-\alpha D}, \text{ for } d < D < D_m \quad (1)$$

can also be written:

$$n = e^{(-\alpha D + b_0)}, \text{ also valid for } d < D < D_m. \quad (2)$$

In either expression, n is the number density of clouds expressed in units of clouds per unit area. In equation (1), K represents the

number density obtained as the cloud base diameter, D , approaches zero. The term e^{b_0} in equation (2) is the equivalent of the term K in equation (1). Essentially, both of these terms are the intercept value determined in the regression analysis. Since the relationships are only valid for values of D which lie in the interval from d to D_m , where d is the smallest cloud diameter observed and D_m is the maximum diameter observed, K and e^{b_0} can be given no physical meaning. The coefficient α is the slope of the regression equation.

If equation (1) is integrated over the range of diameters observed, the total number density of clouds, n_t , representing the sum of the contributions made by all cloud sizes of the sample, can be expressed as:

$$n_t = \int_d^{D_m} n \, dD = \frac{K}{\alpha} \left(e^{-\alpha d} - e^{-\alpha D_m} \right). \quad (3)$$

Since the cloud base cross-sectional area of a single cloud is equal to $\frac{\pi D^2}{4}$, the sky cover distribution function can be written as:

$$s = \left(\frac{\pi D^2}{4} \right) n, \quad (4)$$

and by substitution of equation (1) for n , the decimal sky cover, s , for a group of clouds having diameter D is given by:

$$s = \left(\frac{\pi K D^2}{4} \right) e^{-\alpha D}, \text{ valid for } d < D < D_m. \quad (5)$$

The total sky cover, S_T , consisting of the sum of contributions from all clouds in the diameter range d to D_m is obtained by integrating equation (5) over this range, yielding:

$$S_T = \int_d^{D_m} s \, dD = \frac{\pi K \chi}{2\alpha^3}, \quad (6)$$

$$\text{where } \chi = e^{-\alpha d} \left[\frac{(\alpha d)^2}{2} + \alpha d + 1 \right] - e^{-\alpha D_m} \left[\frac{(\alpha D_m)^2}{2} + \alpha D_m + 1 \right].$$

Equations (1) through (6) are continuous distribution functions and therefore assume an infinitesimal diameter class interval. In order to describe data which has been tabulated in finite class intervals of width ϵ , the previous equations must first be transformed by integrating over the class width.

The number distribution function is now written as:

$$n_f = \int_{D - \frac{\epsilon}{2}}^{D + \frac{\epsilon}{2}} K e^{-\alpha D} \, dD = K \delta_n e^{-\alpha D}, \quad \text{for } d < D < D_m, \quad (7)$$

where

$$\delta_n = \frac{2}{\alpha} \sinh \frac{\alpha \epsilon}{2}, \quad (8)$$

and n_f is the number of clouds within the class width ϵ centered on D .

Equation (5), the sky cover distribution function, becomes:

$$S = \int_{D - \frac{\epsilon}{2}}^{D + \frac{\epsilon}{2}} \frac{\pi K D^2}{4} e^{-\alpha D} \, dD = \left(\frac{\pi K \delta_s}{4} \right) D^2 e^{-\alpha D}, \quad \text{for } d < D < D_m, \quad (9)$$

where

$$\delta_s = \frac{2}{\alpha^3 D^2} \left\{ \left[(\alpha D + 1)^2 + \frac{\alpha^2 \epsilon^2}{4} + 1 \right] \sinh \left(\frac{\alpha \epsilon}{2} \right) - \alpha \epsilon (\alpha D + 1) \cosh \frac{\alpha \epsilon}{2} \right\}. \quad (10)$$

If the value of δ_n in equation (8) is calculated for the specified $\epsilon = 0.96$ km used in the DMSP case studies and for values of α ranging from 0.5 to 2.0 (see Tables 13 through 15), it becomes apparent that δ_n can be approximated by ϵ with less than 10% error. Similar results are obtained in the calculation of values of δ_s from equation (10) if the stipulation that $\alpha D \leq \alpha D_m \leq 9$ is added. The upper limit of the term αD was determined by observations made in the current case studies (see Tables 13 through 15). Therefore, we may simplify equations (7) and (9) by substituting ϵ for both δ_n and δ_s .

If equation (6) is rewritten as:

$$K = \frac{2\alpha^3 S_T}{\pi \chi}, \quad (11)$$

the final form of the number density distribution function becomes:

$$N = \left(\frac{2A_r \epsilon \alpha^3 S_T}{\pi \chi} \right) e^{-\alpha D}, \quad \text{for } d < D < D_m, \quad (12)$$

where

$$N = n_f A_r. \quad (13)$$

In equations (12) and (13), A_r is merely a reference area chosen for normalizing the samples to simplify comparisons. Where n_f was defined previously as the number of clouds per unit area, N is now defined as the number of clouds within the reference area A_r .

Using equation (11) and substituting ϵ for δ_s , the more convenient form for the sky cover distribution function can be written as:

$$S = \left(\frac{\epsilon \alpha^3 S_T}{2\chi} \right) D^2 e^{-\alpha D}, \text{ valid for } d < D < D_m. \quad (14)$$

Also, equation (11) can be used in equation (3) to transform the total number density equation into its final form:

$$N_T = \left(\frac{2A_r \alpha^2 S_T}{\pi\chi} \right) \left(e^{-\alpha d} - e^{-\alpha D_m} \right), \quad (15)$$

where

$$N_T = n_t A_r. \quad (16)$$

As in equation (13), A_r is the reference area used in normalizing the data. Since n_t was defined as the total number of clouds per unit area, N_T is defined by equation (16) as the total number of clouds over the reference area A_r .

Equations (12), (14), and (15) will be evaluated in chapter three using the observed diameter ranges seen in Tables 13 through 15, the observed total sky cover, S_T , and the value of α determined by the regression analysis performed on a linearized form of the exponential model.

1.4 Satellite Applicability

Most ground-based observation sites cannot accurately measure the parameters discussed in the previous section. Due to the curvature of the earth, an observer can only estimate the total sky cover overhead within a few miles of the station. Plank (1969) estimates that the report of a ground observer is only representative of an area of approximately 20 km^2 .

Airborne observation platforms, used to gather photographic or radar data, are one answer to the problem of obtaining data which is representative of a larger area. There are several drawbacks to aircraft operation, however. One limitation is the airspeed of the aircraft gathering the data. If an extremely large field of clouds is the subject of investigation, it would be impossible for a single aircraft to view the entire field simultaneously. If many aircraft are used, or if the research project is carried out over an extended period of time, the cost of aircraft operation becomes prohibitive.

Prior to the early 1970's, the resolution of meteorological satellites was too crude to adequately detect the individual clouds of a field. With the advent of the current generation satellites, however, data resolution has improved to the point that objects of 0.6 km horizontal extent can be detected. The use of a sun-synchronous satellite platform allows the researcher to monitor several geographic areas that are separated by thousands of miles without the duplication of effort required by ground-based or airborne systems. In addition to visual coverage of the earth scene, high resolution infrared sensors allow the analyst to infer the temperature, and therefore the heights, of the cloud tops.

Due to the distance between sampling areas and the length of time over which the data was gathered for the current study, the analysis of satellite data was the only economical way of investigating the size distributions of small cumulus clouds.

2.0 SAMPLING PROCEDURE

2.1 Selection of Data

The satellite imagery chosen for the case studies was obtained from two vehicles.

The first source of data was vehicle number 5528 of the Defense Meteorological Satellite Program (DMSP). Satellites in this program fly in a circular orbit at a nominal altitude of 450 nm (830 km) and an inclination angle of 98.7 degrees, ensuring an orbit that will remain sun-synchronous. The chosen vehicle had an ascending nodal crossing near noon local sun time.

There are two types of visual data available from DMSP vehicles. High resolution visual (HR) data has a resolution of 3.7 km at satellite subtrack. Very high resolution visual (VHR) imagery has a resolution of 0.6 km at subpoint. The VHR data was utilized for the case studies due to the anticipated size spectrum of cumulus under investigation.

The second source of data used in this study was the SMS-1 vehicle. The SMS-1 is a geosynchronous satellite which maintains an altitude of approximately 35,700 km. The data has a nominal resolution of 0.9 km at satellite subpoint, which remained at 1.5°N, 45°W during all days examined.

2.2 Data Processing

The DMSP data were provided by the University of Wisconsin in the form of positive transparencies. Diazo copies, similar to matte finished photographs, were made from the transparencies. The diazo

method of copying was chosen for its simplicity and economy. The process consists of two easy steps. First, a transparency and a piece of specially treated paper are inserted in an ozalid machine, exposing the paper to an ultraviolet lamp which shines through the transparency. The transparency and exposed paper then leave the machine. Step two begins when the exposed paper is reinserted in the upper half of the machine, where it is bathed in ammonia vapor. The ammonia bath brings out the latent image and stops any further reaction on the paper. The contrast of the print can be changed by experimentally varying the times of exposure and ammonia bath. The quality of the finished product can rival that of a photograph if a high quality reproduction paper, such as GAF 102Z, is used in this process.

Next, the diazo copies had to be gridded in order to accurately locate the areas to be studied. A computer generated universal grid was used in this process. It is universal in that a single grid can be used for all pictures. The latitude circles are labeled, but the meridians are purposely left unlabeled. To grid the pictures, a minimum of two prominent land features were found in the vicinity of each case study area. The grid was then placed over the picture with the centerlines of both the grid and picture aligned. The grid was then shifted north or south until the latitudes of the chosen features matched the appropriate latitude circle on the grid. Knowing the longitudes of the land features, one can then apply temporary labels to the meridians on the grid. By selecting a third land feature, the accuracy of the gridding can be quickly checked. If care is taken

during the gridding process, accuracy in locating a point is on the order of 10 to 15 km.

If convenient land features are not present or are obscured by cloud masses, another method of gridding must be employed. This method, described adequately by Dickinson, et al. (1974), was not employed in the processing of data contained in this report.

The SMS-1 data were obtained in the form of 23 cm by 27 cm contact photographs. Since these prints were gridded before printing, the two steps mentioned above were eliminated in processing these data for analysis.

The final step in processing the data for analysis was the preparation of an acetate overlay outlining the area to be studied. Plank (1969) recommends that an area $>2600 \text{ km}^2$ be used to obtain a representative sample from afternoon populations of small cumulus. For this reason, the dimensions of the rectangle used to outline the study areas were chosen to be one degree latitude by one degree longitude. Near the equator such dimensions would result in an area of approximately $1.200 \times 10^4 \text{ km}^2$. The precise dimensions represented by the rectangle were obtained from the Smithsonian Meteorological Tables (1971).

2.3 Equipment

Since the cloud images on the data were on the order of $2.5 \times 10^{-1} \text{ mm}$, a magnifying lens was used to enlarge the images for analysis. The lens employed was a five power magnifying glass attached to a stand which kept the lower face of the lens approximately

3.8 cm above the data. This allowed ample room to work beneath the lens and also left one hand free to tabulate the data.

A precision engineering rule was used to measure the dimensions of the cloud images. The rule was graduated in .01 inch increments which, when magnified by the lens, made estimates of .005 inches possible. Use of the rule and lens was then tested to obtain an estimate of the error to be expected when analyzing the data. Several small and features were measured from the satellite imagery. These same features were then measured on detailed navigation charts and the results were compared. For features less than 4 km in size, the errors ranged from 1.3% to 16.0% with a mean error of 10.1%. Errors in measuring features between 19 km and 55 km ranged from 4.3% to 16.9% with a mean error of 8.2%.

The last piece of equipment needed to analyze the data was a mask made of heavy manilla paper. The mask reduced the analysis area to 1400 km² parcels. After analysis within the exposed data parcel was completed, the mask was shifted to expose a new area of data for analysis. By covering those areas of the imagery that had already been studied, redundancy in tabulating the data was effectively eliminated.

2.4 Automated Sampling

An attempt was made to automate the sampling and tabulating procedures. The optical data digitizer and display system (OD³) was used in order to automate the task of sampling. The digitizing techniques described by Stodt and Grant (1976) were used with only moderate success. The primary drawback encountered in using the OD³

was the inability of the machine to properly represent the smallest clouds in a field. There was a tendency for the machine to eliminate up to 50% of the smaller clouds simply by area-averaging the brightness values of the cloud and the background. Some suggestions for improving the results obtained from the OD³ will be offered in chapter four.

There was no adequate computer software available to tabulate the digitized data. A pattern-recognition type of program would have to be developed before the computer could discern clouds from background brightness variations, noise in the satellite data, and OD³ system noise. Since the current investigation was conducted as a feasibility study, it was felt that such an extensive programming effort was not justified at this time. Given the proper computer software, however, the process could easily be automated with the computer products yielding additional information, such as albedos and cloud separation distances.

3.0 CASE STUDIES

3.1 Data Sets

Ninety-three quarter orbits of DMSP imagery covering the eastern United States were obtained for the period 1 June 1973 to 31 August 1973. These data were then examined in conjunction with surface synoptic charts to find areas which were relatively undisturbed. The subset consisting of data which met this requirement were next subjected to the following criteria:

1. Areas containing major topographic features such as the Appalachian Mountains were eliminated since the physical mechanism for orographic cloud formation was felt to be too unlike the mechanism for convective cumulus formation.
2. Areas near the edge of the DMSP imagery were eliminated due to inherent higher distortion and poorer resolution.
3. Imagery containing excessive data gaps or other system noise were discarded to minimize data contamination. In many instances a small cumulus can not be distinguished from the image produced by a burst of electronic noise.
4. Samples containing more than one layer of clouds were not considered as candidates for case studies. The worst offender in this category was thin cirrus overlying a field of small cumulus. The cirrus acts to reduce the contrast between the individual cumulus cell and the surface, making measurements both tedious and unreliable.

Imagery which remained after being subjected to the preceding elimination procedure were considered for case studies. Three case study areas were finally selected from the DMSP data: North Carolina, Florida, and an oceanic data set. A second oceanic case study area in the eastern Atlantic was chosen from the SMS-1 data.

3.1.1 North Carolina

Five samples were taken from eastern North Carolina in an area bounded by 35°N, 36°N, 77°W, and 78°W shown in Figure 1. The dates and DMSP imagery used for the data set are summarized in Table 1.

Table 1. North Carolina Case Study

Date	Orbit Number	Ascending Node Time (GMT)
2 June 73	6157	1640
5 June 73	6200	1738
10 July 73	6695	1737
20 July 73	6836	1633
21 July 73	6850	1639

The cumulus clouds within the sampling area were measured and tabulated by size. The class width chosen for data tabulation was approximately 0.96 km, the smallest increment which could be reliably estimated by the analyst. Since the area covered by clouds varied from sample to sample, the number of clouds in each size category was normalized by the following relationship:

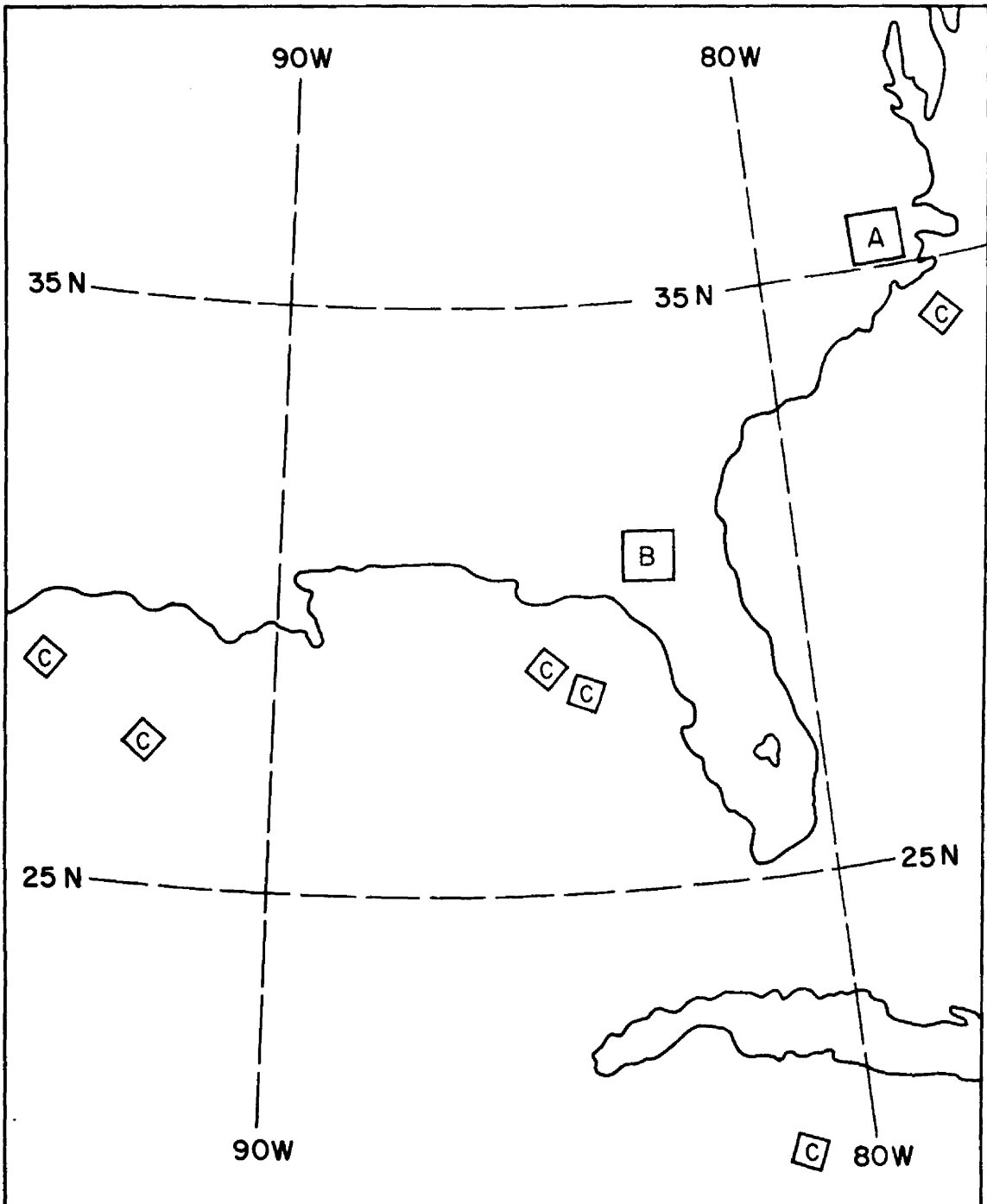


Figure 1. Locations of DMS Case Studies.

(A - North Carolina sampling area.
B - Florida sampling area.
C - Oceanic sampling areas.)

$$n_i = \frac{n_o}{A_c \times 10^{-3}},$$

where n_i is the number of clouds per 1000 km², n_o is the number of clouds observed in a given class interval, and A_c represents the area within the sampling boundaries that was cloud covered. The normalized cloud number density values, n_i , allowed comparisons between samples and other case study areas. The normalized number densities for five samples comprising the North Carolina case study are shown in Table 2. The mean cloud number densities were also plotted as a histogram as shown in Figure 2. The dashed line in the figure is a plot of the regression equation $\ln \bar{n} = -0.9048 D + 3.8842$, where \bar{n} is the predicted mean cloud number density and D is any cloud diameter in the range from 0.6 km to 9.5 km.

The contribution made by each size class to the total sky cover within the sampling area was computed using the relationship $s_i = \frac{D_i^2 n_i}{4A_r}$, where s_i is the decimal sky cover contribution made by the i^{th} class of clouds, $\frac{\pi D_i^2}{4}$ is the cross-sectional area of the base of a single cumulus in the i^{th} class, n_i is the observed (normalized) cloud number density, and A_r is the reference area used in normalizing, i.e. 1000 km². The decimal sky cover contributions for the North Carolina samples are listed in Table 3 and the mean values plotted as a histogram in Figure 3. The small squares plotted on the histogram indicate the theoretical sky cover distribution $S = \left(\frac{\epsilon \alpha^3 S_T}{2\chi} \right) D^2 e^{-\alpha D}$ as discussed in section 1.3.

Table 2. Normalized Cloud Number Density,
North Carolina Samples.

Date	Cloudy Area, A_c , km^2	Equivalent Cloud Diameter, km									
		0.96	1.91	2.87	3.82	4.78	5.72	6.69	7.63	8.59	9.54
2 June 73	9190	15.7	10.8	3.65	1.58	0.438	0.111	0	0	0	0
5 June 73	10700	12.7	10.5	3.94	2.53	1.59	0.937	0.280	0	0.093	0
10 July 73	10700	13.8	10.6	7.30	3.10	1.50	0.654	0.187	0.093	0	0.093
20 July 73	7610	21.1	13.7	3.71	1.19	0.199	0	0	0	0	0
21 July 73	9160	16.0	8.15	1.26	0.493	0.055	0.055	0	0	0	0
Mean	9472	15.9	10.7	3.97	1.77	0.756	0.350	0.093	0.018	0.018	0.018

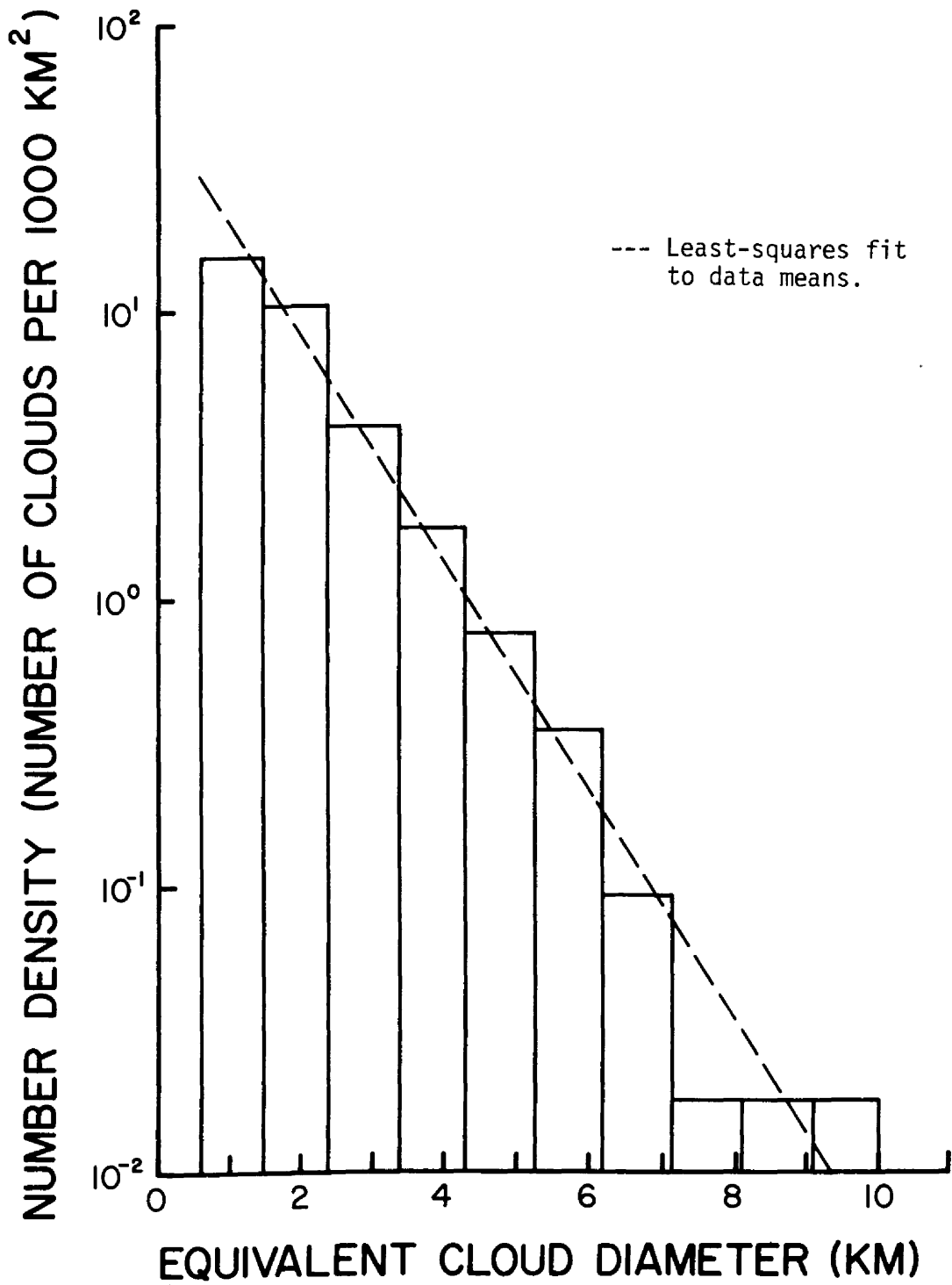


Figure 2. North Carolina Case Study.

Table 3. Contributions to Total Sky Cover,
North Carolina Samples.

Date	Equivalent Cloud Diameter, km										Total
	0.96	1.91	2.87	3.82	4.78	5.72	6.69	7.63	8.59	9.54	
2 June 73	0.0114	0.0308	0.0236	0.0180	0.0078	0.0028	0	0	0	0	0.0944
5 June 73	0.0093	0.0299	0.0254	0.0288	0.0285	0.0240	0.0098	0	0.0054	0	0.1611
10 July 73	0.0101	0.0286	0.0472	0.0352	0.0268	0.0168	0.0066	0.0043	0	0.0067	0.1823
20 July 73	0.0154	0.0391	0.0240	0.0135	0.0036	0	0	0	0	0	0.0956
21 July 73	0.0117	0.0232	0.0081	0.0056	0.0010	0.0014	0	0	0	0	0.0510
Mean	0.0116	0.0303	0.0257	0.0202	0.0135	0.0090	0.0033	0.0009	0.0011	0.0013	0.1169

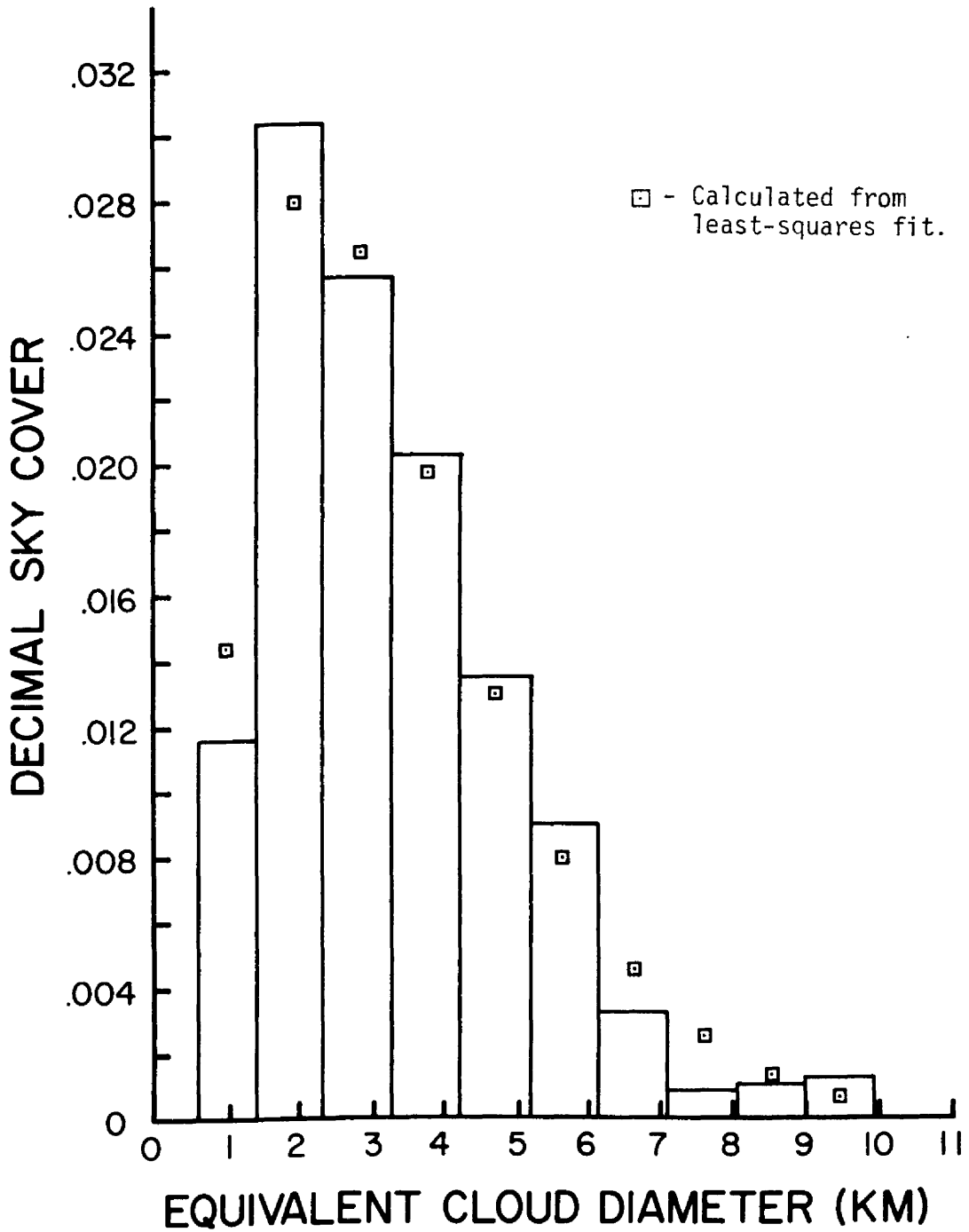


Figure 3. Observed Mean Sky Cover Contributions, North Carolina Case Study.

3.1.2 Florida

A second continental sampling area was chosen over northern Florida, bounded by 30°N, 31°N, 82.5°W, and 83.5°W. The location of the area can be seen in Figure 1. The DMSP imagery selected for the case study has been summarized in Table 4. The data tabulation and normalization methods were identical to those used in the North Carolina case study. The normalized cloud number density results are

Table 4. Florida Case Study

Date	Orbit Number	Ascending Node Time (GMT)
4 June 73	6186	1753
14 June 73	6327	1709
9 August 73	7119	1707
10 August 73	7133	1653
20 August 73	7275	1750
30 August 73	7416	1706

compiled in Table 5. The mean cloud number densities are also shown as a histogram in Figure 4. The dashed line in the figure is a plot of the regression equation $\ln \bar{n} = -0.7956 D + 3.1029$, which is valid for values of D in the interval from 0.6 km to 10.5 km.

Contributions to the total sky cover of each sample were computed and are listed in Table 6. The mean decimal sky cover contributions are plotted in Figure 5, with the theoretical sky cover distribution being represented by small squares.

Table 5. Normalized Cloud Number Density,
Florida Samples.

Date	Cloudy Area, A_c , km^2	Equivalent Cloud Diameter, km										
		0.96	1.91	2.87	3.82	4.78	5.72	6.69	7.63	8.59	9.54	10.48
4 June 73	11095	32.7	13.3	3.88	2.62	0.362	0.272	0	0	0	0	0
14 June 73	9725	17.7	7.1	1.54	0.619	0.207	0.310	0	0	0	0	0
9 Aug. 73	10030	17.3	12.2	1.70	0.099	0	0	0	0	0	0	0
10 Aug. 73	9175	12.4	6.45	2.84	1.09	0.219	0.108	0.108	0	0	0	0
20 Aug. 73	8335	17.3	3.97	0	0	0	0	0	0	0	0	0
30 Aug. 73	11200	24.6	12.4	4.47	2.06	0.715	0.447	0.091	0.178	0.091	0.091	0.091
Mean	9927	20.3	9.23	2.41	1.08	0.251	0.190	0.032	0.030	0.015	0.015	0.015

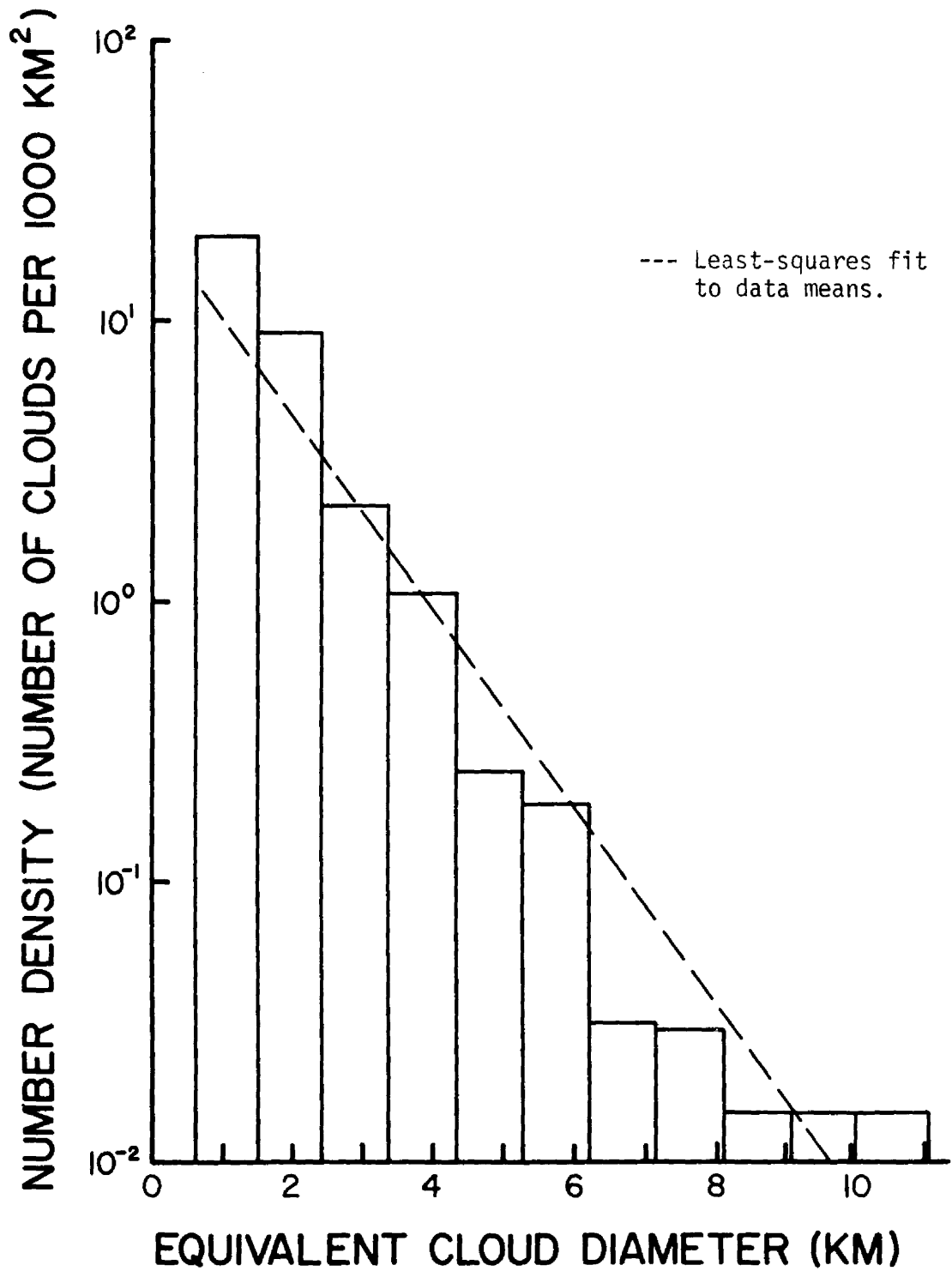


Figure 4. Florida Case Study.

Table 6. Contributions to Total Sky Cover,
Florida Samples.

Date	Equivalent Cloud Diameter, km											Total
	0.93	1.91	2.87	3.82	4.78	5.72	6.69	7.63	8.59	9.54	10.48	
4 June 73	0.0238	0.0382	0.0250	0.0298	0.0065	0.0069	0	0	0	0	0	0.1302
14 June 73	0.0128	0.0202	0.0099	0.0071	0.0037	0.0079	0	0	0	0	0	0.0616
9 Aug. 73	0.0126	0.0347	0.0110	0.0011	0	0	0	0	0	0	0	0.0594
10 Aug. 73	0.0090	0.0183	0.0183	0.0125	0.0039	0.0028	0.0037	0	0	0	0	0.0685
20 Aug. 73	0.0125	0.0113	0	0	0	0	0	0	0	0	0	0.0238
30 Aug. 73	0.0179	0.0352	0.0289	0.0235	0.0128	0.0115	0.0031	0.0082	0.0052	0.0012	0.0077	0.1552
Mean	0.0148	0.0263	0.0155	0.0123	0.0045	0.0049	0.0011	0.0014	0.0009	0.0002	0.0013	0.0832

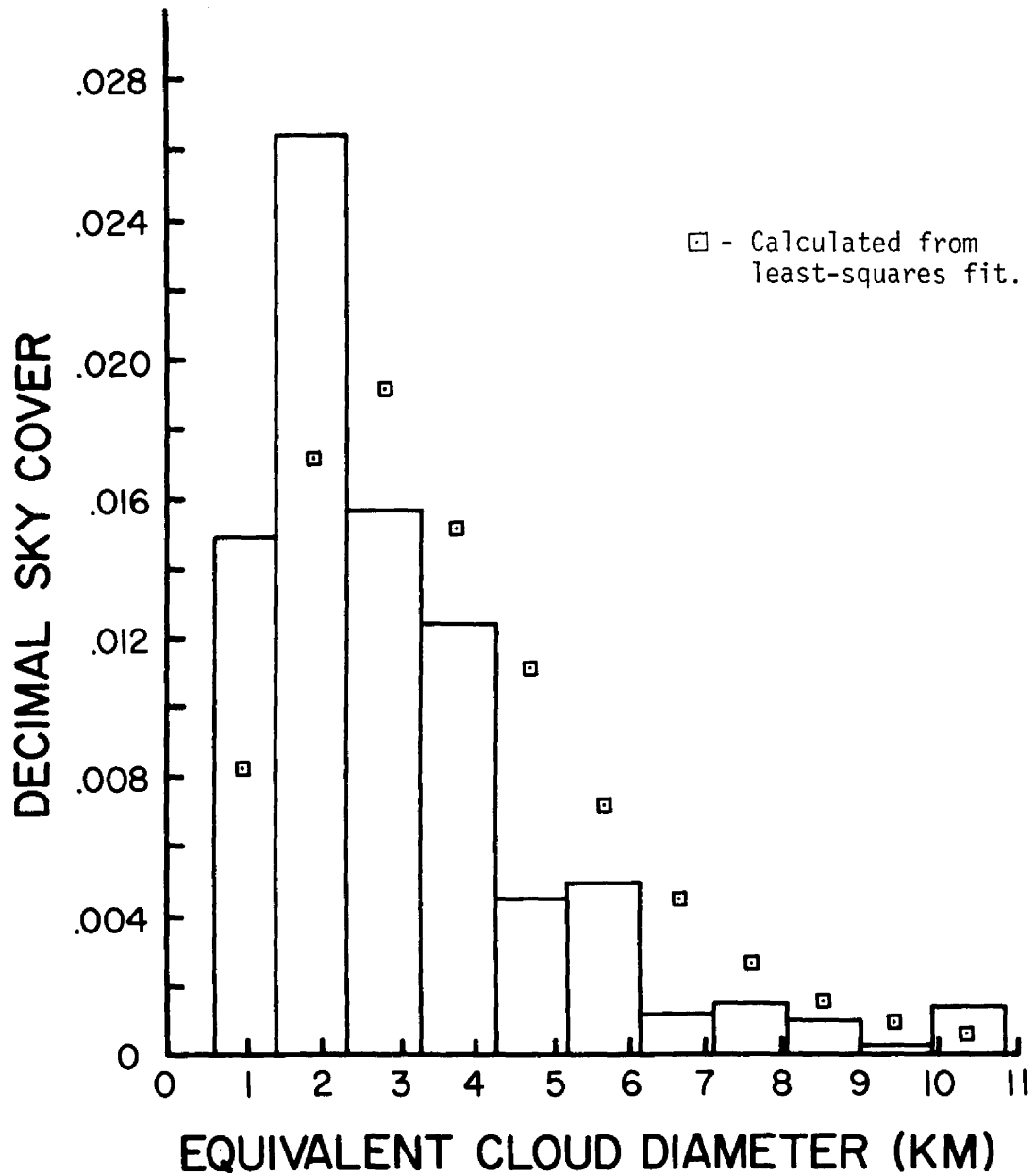


Figure 5. Observed Mean Sky Cover Contributions, Florida Case Study.

3.1.3 DMSP Oceanic

Six samples of maritime cumulus populations were included in the DMSP oceanic case study. Because topography is not of concern in choosing oceanic sampling areas, the samples were not required to be colocated as they were in the previous case studies. Four samples were taken from the Gulf of Mexico, one sample from the Western Atlantic Ocean, and one sample from the Caribbean Sea. The relative locations of the samples can be seen in Figure 1. Exact geographic coordinates, along with information concerning DMSP data used, are summarized in Table 7.

Normalized cloud number densities were calculated using the same techniques as the previous two case studies. The number densities, n_i , or number of clouds per 1000 km^2 are presented in Table 8. The mean number densities were then plotted (see Figure 6) and a regression line was calculated to be $\ln \bar{n} = -0.9789 D + 3.4135$. The least-squares fit to the data is shown in Figure 6 as a dashed line, and is valid for values of D between 0.6 km and 7.63 km.

Observed sky cover contributions made by each class interval are listed in Table 9. The mean sky cover contribution of each class was then computed and plotted (see Figure 7). The theoretical sky cover distribution values, obtained from the relationship $S = \left(\frac{\epsilon \alpha^3 S_T}{2\chi} \right) D^2 e^{-\alpha D}$, are plotted on the figure as small squares.

3.1.4 SMS-1 Oceanic

A second oceanic case study was compiled from the 0.9 km resolution SMS-1 satellite imagery. Seven samples were taken in the eastern

Table 7. DMSP Oceanic Case Study

Date	Orbit Number	Ascending Node Time (GMT)	Location of Sampling Boundaries			
16 July 73	6780	1751	29.1 N/85.0 W	28.8 N/84.5 W	28.3 N/85.0 W	28.7 N/85.5 W
17 July 73	6793	1737	21.0 N/81.3 W	20.8 N/80.8 W	20.3 N/81.0 W	20.4 N/81.4 W
18 July 73	6808	1722	34.0 N/77.0 W	34.4 N/76.4 W	34.0 N/75.9 W	33.6 N/76.6 W
30 July 73	6978	1751	29.0 N/94.5 W	28.7 N/94.0 W	28.2 N/94.3 W	28.4 N/94.8 W
20 Aug. 73	7275	1750	27.8 N/92.4 W	27.4 N/91.9 W	26.9 N/92.3 W	27.3 N/92.9 W
29 Aug. 73	7402	1721	28.5 N/84.5 W	28.4 N/84.0 W	27.8 N/84.1 W	27.9 N/84.6 W

Table 8. Normalized Cloud Number Density, DMSP Oceanic Samples.

Date	Location	Cloudy Area, A_C , km ²	Equivalent Cloud Diameter, km							
			0.96	1.91	2.87	3.82	4.78	5.72	6.69	7.63
16 July 73	Gulf of Mexico	2830	15.6	7.07	1.06	0.353	0.353	0	0	0
17 July 73	Caribbean	2315	22.5	3.47	2.16	0	0	0	0	0
18 July 73	Atlantic	3340	27.0	11.1	2.40	0.899	0	0	0	0
30 July 73	Gulf of Mexico	3600	20.0	10.6	3.07	2.78	0	0	0	0
20 Aug. 73	Gulf of Mexico	3430	16.9	4.09	2.34	0.584	0	0	0	0.292
29 Aug. 73	Gulf of Mexico	3260	19.7	8.29	1.23	0.307	0	0	0	0
Mean		3129	20.3	7.42	2.04	0.403	0.058	0	0	0.050

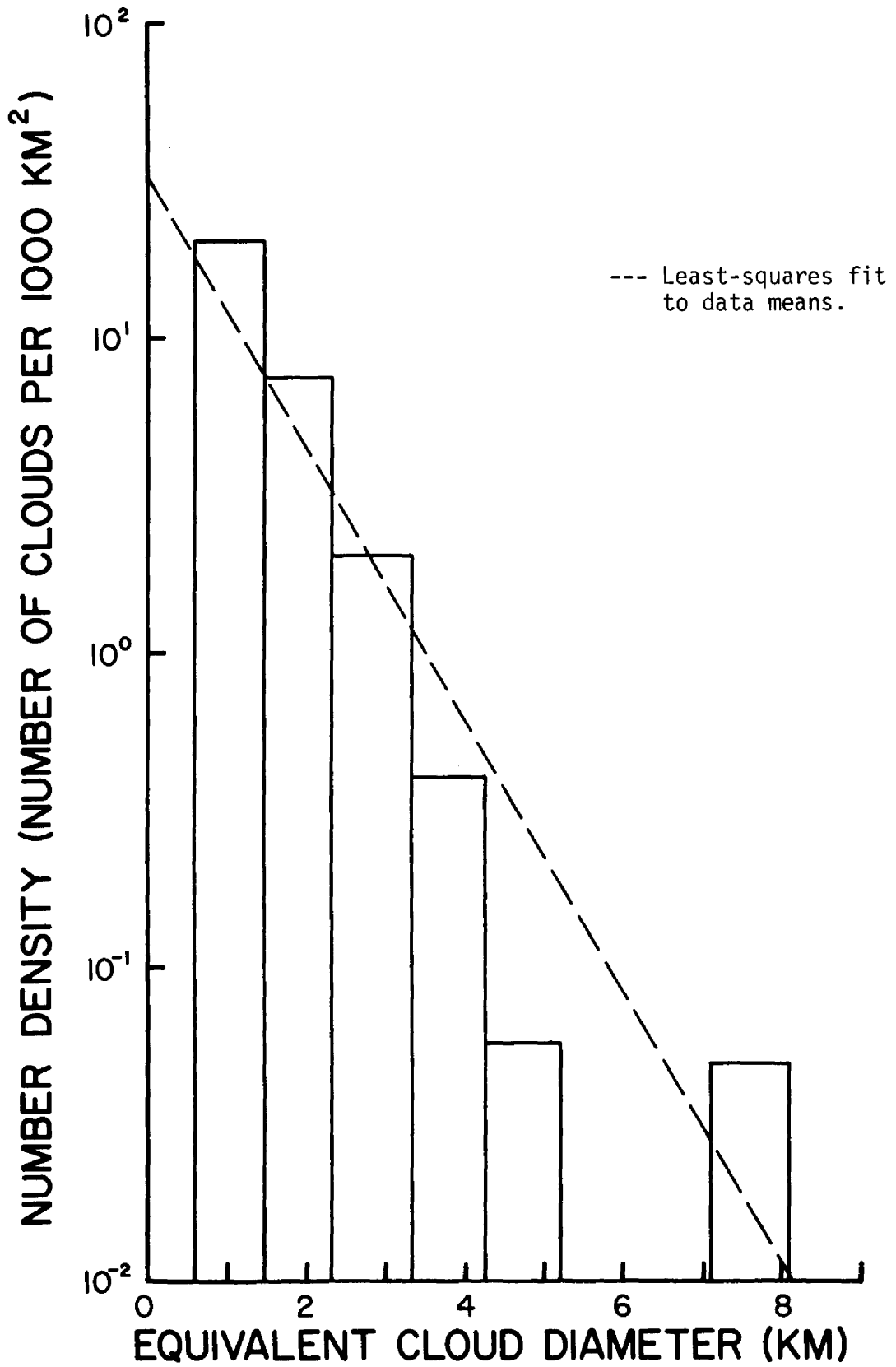


Figure 6. DMSP Oceanic Case Study.

Table 9. Contributions to Total Sky Cover, DMSP Oceanic Samples.

Date	Location	Equivalent Cloud Diameter, km								
		0.96	1.91	2.87	3.82	4.78	5.72	6.69	7.63	Total
16 July 73	Gulf of Mexico	0.0113	0.0202	0.0069	0.0040	0.0063	0	0	0	0.0487
17 July 73	Caribbean	0.0164	0.0099	0.0140	0	0	0	0	0	0.0403
18 July 73	Atlantic	0.0196	0.0316	0.0155	0.0103	0	0	0	0	0.0770
30 July 73	Gulf of Mexico	0.0146	0.0302	0.0198	0.0032	0	0	0	0	0.1992
20 Aug. 73	Gulf of Mexico	0.0123	0.0117	0.0151	0.0067	0	0	0	0.0133	0.0591
29 Aug. 73	Gulf of Mexico	0.0143	0.0237	0.0079	0.0035	0	0	0	0	0.0494
Mean		0.0148	0.0212	0.0132	0.0046	0.0011	0	0	0.0022	0.0571

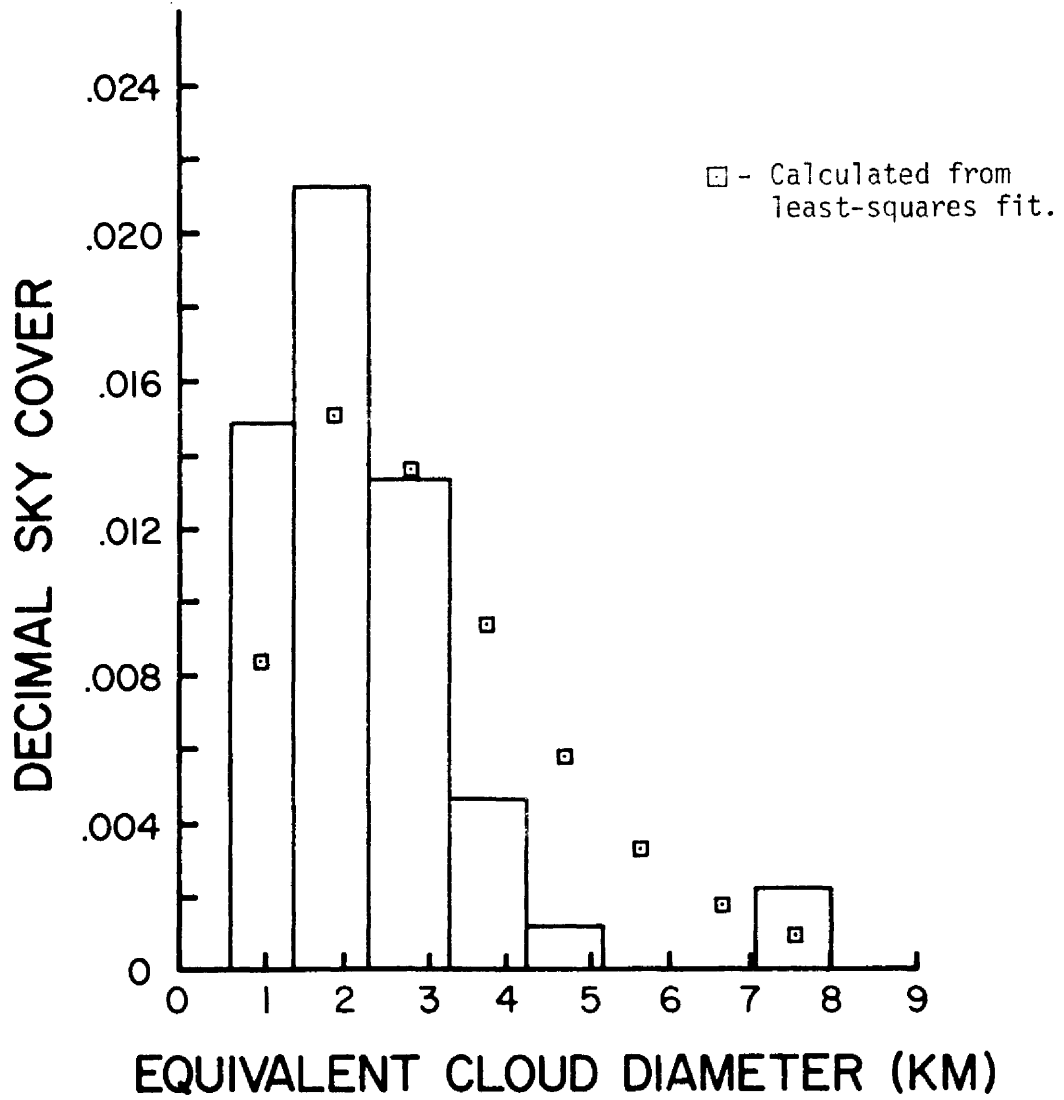


Figure 7. Observed Mean Sky Cover Contributions, DMSP Oceanic Case Study.

Atlantic Ocean in the vicinity of the GATE A-B scale ship array (see Figure 8). The numbers beside each sample indicate the Julian date of the sample. Additional information concerning the SMS-1 data used for the case study can be found in Table 10.

Data tabulation methods for this case study were modified slightly due to the change in data source. Since SMS-1 imagery is not produced at the same scale as DMSP data, a new scale conversion factor had to be computed before tabulation could proceed. An image which measures 0.01 inch on SMS-1 data represents an object that has a dimension of 1.5 km. The class interval was therefore chosen to be 0.75 km, the smallest increment that could be estimated. The reference area used in normalizing the results remained unchanged at 1000 km². The normalized cloud number density results are presented in Table 11. The mean number density for each class interval was calculated and plotted as the histogram seen in Figure 9. The least-squares fit to the data was computed as $\ln \bar{n} = -0.5981D + 1.9511$, valid for 1.1 km < D < 10.4 km, and is seen in the figure as a dashed line.

The cloud cover contributions made by each class interval to the total sky cover are listed in Table 12. Mean contributions were then plotted (see Figure 10) and a theoretical sky cover distribution was computed. Theoretical contributions are plotted on the figure as a small square for each class interval.

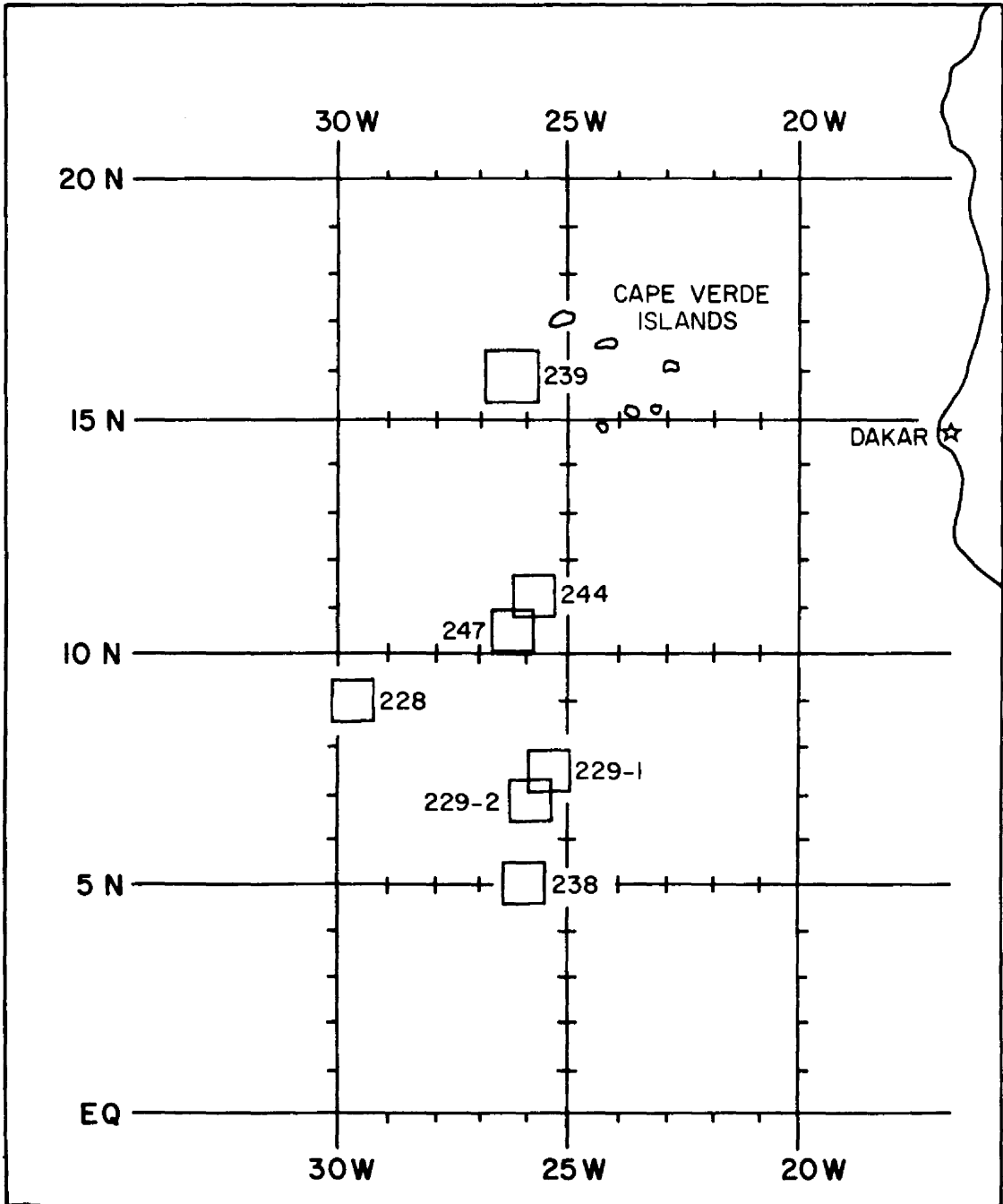


Figure 8. Locations of SMS-1 Sampling Areas.

Table 10. SMS-1 Oceanic Case Study.
 (All samples taken at 1300 GMT.)

Date	Julian Date (- Sample Number)	Location of Sampling Boundaries			
16 Aug. 74	228	9.5 N/30.3 W	9.5 N/29.3 W	8.5 N/29.3 W	8.5 N/30.3 W
17 Aug. 74	229-1	8.0 N/26.0 W	8.0 N/25.0 W	7.0 N/25.0 W	7.0 N/26.0 W
17 Aug. 74	229-2	7.3 N/26.3 W	7.3 N/25.3 W	6.3 N/25.3 W	6.3 N/26.3 W
26 Aug. 74	238	5.5 N/26.5 W	5.5 N/25.5 W	4.5 N/25.5 W	4.5 N/26.5 W
27 Aug. 74	239	16.4 N/26.9 W	16.4 N/25.9 W	15.4 N/25.9 W	15.4 N/26.9 W
1 Sep. 74	244	11.8 N/26.3 W	11.8 N/25.3 W	10.8 N/25.3 W	10.8 N/26.3 W
4 Sep. 74	247	11.0 N/26.8 W	11.0 N/25.8 W	10.0 N/25.8 W	10.0 N/26.8 W

Table 11. Normalized Cloud Number Density,
SMS-1 Oceanic Samples.

Julian Date	Cloudy Area, A_c , km ²	Equivalent Cloud Diameter, km												
		1.5	2.2	3.0	3.7	4.4	5.2	5.9	6.7	7.4	8.2	8.9	9.6	10.4
228	9740	1.88	2.24	1.18	0.590	0.823	0.117	0.117	0	0	0.117	0	0	0
229-1	9880	2.33	1.52	1.01	0.201	0.304	0	0.102	0	0	0	0	0	0
229-2	11230	3.04	1.61	0.891	0.178	0.091	0	0	0	0	0	0	0	0
238	4890	1.44	1.64	1.85	0.821	1.44	0	0.204	0.409	0	0.204	0	0	0
239	11270	4.91	3.12	2.05	1.60	0.800	0	0.266	0.088	0	0	0	0	0
244	8335	0.602	1.20	1.20	0.841	1.08	0.961	0.721	0.602	0.359	0	0	0	0.120
247	9430	3.50	2.01	1.70	0.637	0.742	0.423	0.318	0	0	0	0	0	0
Mean	9254	2.53	1.90	1.41	0.695	0.753	0.213	0.248	0.158	0.053	0.047	0	0	0.017

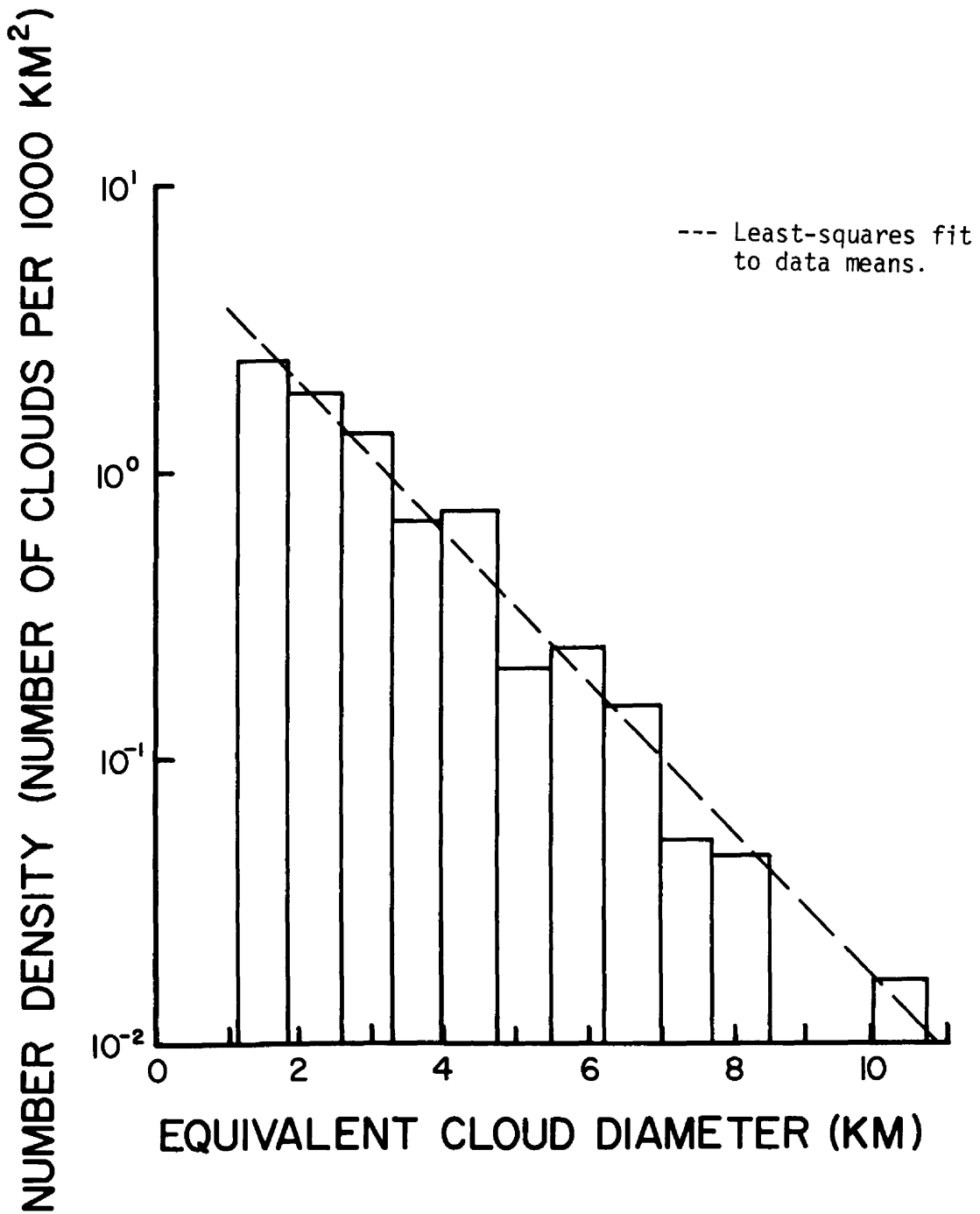


Figure 9. SMS-1 Oceanic Case Study.

Table 12. Contributions to Total Sky Cover,
SMS-1 Oceanic Samples.

Julian Date	Equivalent Cloud Diameter, km													Total
	1.5	2.2	3.0	3.7	4.4	5.2	5.9	6.7	7.4	8.2	8.9	9.6	10.4	
228	0.0032	0.0087	0.0081	0.0063	0.0128	0.0025	0.0032	0	0	0.0061	0	0	0	0.0509
229-1	0.0040	0.0059	0.0070	0.0022	0.0047	0	0.0028	0	0	0	0	0	0	0.0266
229-2	0.0052	0.0062	0.0061	0.0019	0.0014	0	0	0	0	0	0	0	0	0.0208
238	0.0025	0.0064	0.0127	0.0088	0.0222	0	0.0056	0.0143	0	0.0107	0	0	0	0.0832
239	0.0084	0.0121	0.0141	0.0172	0.0124	0	0.0073	0.0031	0	0	0	0	0	0.0746
244	0.0010	0.0047	0.0083	0.0090	0.0167	0.0203	0.0198	0.0209	0.0155	0	0	0	0.0101	0.1263
247	0.0060	0.0078	0.0117	0.0068	0.0115	0.0089	0.0088	0	0	0	0	0	0	0.0615
Mean	0.0043	0.0074	0.0097	0.0075	0.0117	0.0045	0.0068	0.0055	0.0022	0.0024	0	0	0.0014	0.0634

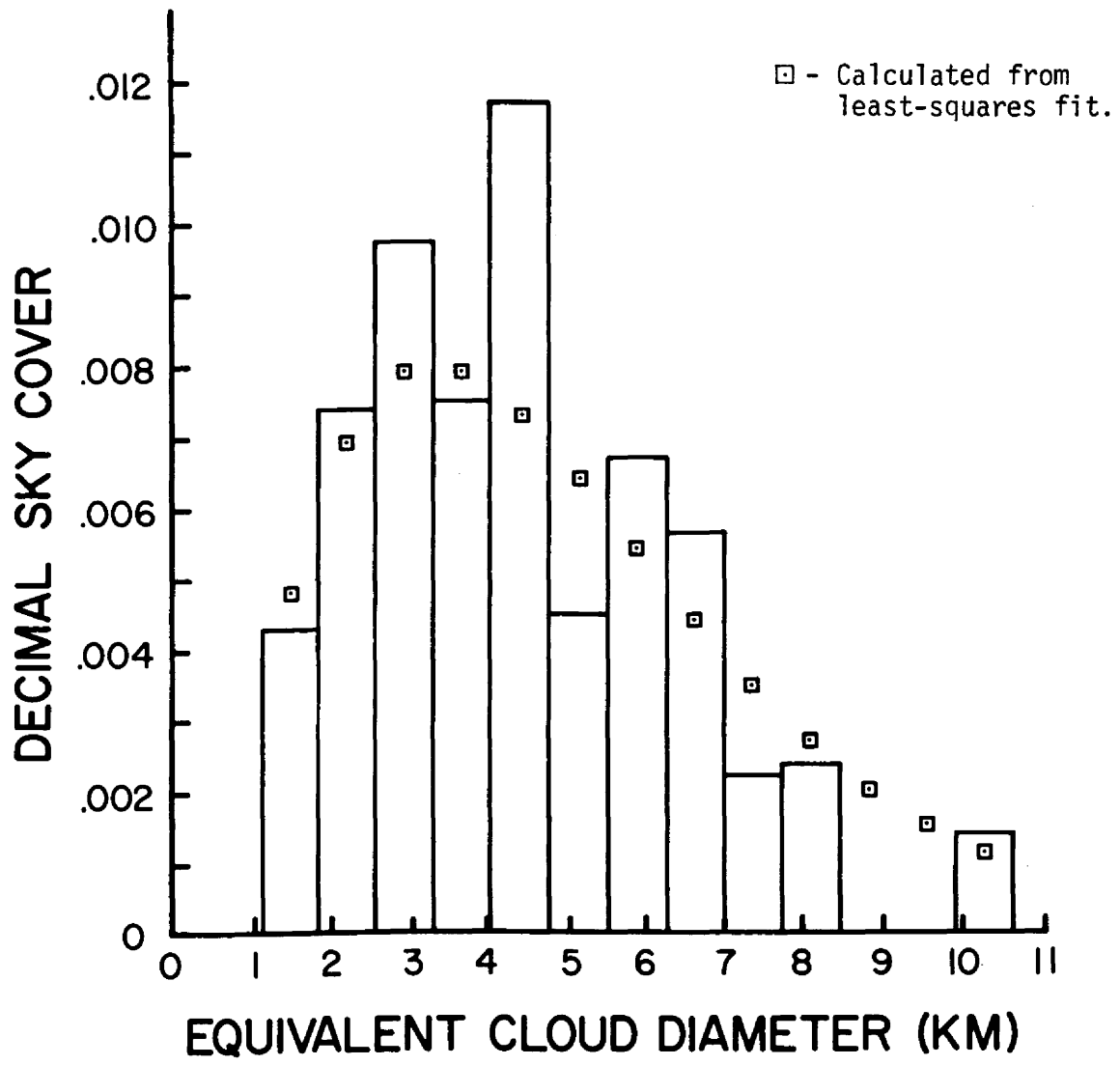


Figure 10. Observed Mean Sky Cover Contributions, SMS-1 Oceanic Case Study.

3.2 Discussion

3.2.1 Comparison of Case Studies

Observed and theoretical values for population parameters of the four case studies have been compiled in Table 13 in order to facilitate a discussion of the results.

In comparing the two continental case study areas, many similarities in the parameters can be seen. In both case studies the smallest diameter clouds observed were 0.6 km, the limit imposed by the resolution of the satellite imagery. The largest diameter clouds, D_m , were between 9.5 km and 10.5 km for both case studies. The observed total number density, N_T , in number of clouds per 1000 km^2 was found to be identical. The observed parameter N_T was obtained by summing the individual mean number density values found at the bottom of Tables 2 and 5. The theoretical value of N_T was then calculated from the expression $N_T = \left[\frac{2A_r \alpha^2 S_T}{\pi X} \right] \left(e^{-d} - e^{-D_m} \right)$, discussed in chapter 1.3. The agreement of the observed and calculated N_T values is a measure of how well the regression equation fits the data in the first few counting intervals, where the greatest contributions to N_T are made. The North Carolina data shows good agreement between the two values of N_T , indicating a good fit of the regression line to the observed data (see Figure 2). The data gathered in the Florida case study did not fare as well, having a theoretical value of N_T 38% lower than the observed value. This indicates a poorer fit of the regression equation in the smaller diameter classes. Figure 4 shows that the regression equation predicts too small a contribution in the first two class intervals.

Table 13. Summary of Case Study Parameters.

Case Study	d (km) Observed	D_m (km) Observed	N_T Observed	N_T Theoretical	S_T Observed	S_T Theoretical	α (km^{-1})	αD_m	χ	D' (km)
North Carolina	0.6	9.54	34	36	0.1169	0.1142	0.9048	8.63	0.972	2.20
Florida	0.6	10.48	34	21	0.0832	0.0871	0.7956	8.39	0.976	2.43
DMSO Oceanic	0.6	7.63	30	20	0.0571	0.0574	0.9789	7.47	0.956	2.04
SMS-1 Oceanic	1.1	10.40	8	8	0.0628	0.0618	0.5981	6.22	0.940	3.33

The observed values of S_T , the total sky cover, were found by summing the mean contributions listed at the bottom of Tables 3 and 6. The theoretical total sky cover values were calculated using the expression $S_T = \sum S$, where $S = \left[\frac{\epsilon \alpha^3 S_T}{\pi \chi} \right] D^2 e^{-D}$. The agreement between the observed and theoretical values of S_T were quite good in both case studies. The theoretical total sky cover for the North Carolina case study was in error by 2.3%; the theoretical S_T value for the Florida case study was in error by 4.7%.

The slope of the regression line, α , is seen to be slightly greater for the North Carolina data than for the Florida data. This is caused by the inclusion of cloud group structures in the regression analysis. The effect of eliminating group structures will be discussed in the next section of this paper.

The cloud diameter yielding the maximum contribution to sky cover, denoted by D' , is obtained by differentiating the distribution equation $s = \left[\frac{\pi K D^2}{4} \right] e^{-\alpha D}$ with respect to D and setting $\frac{ds}{dD}$ equal to zero. The resulting diameter, $D' = \frac{2}{\alpha}$, should not be expected to agree precisely with the modal diameters shown in Figures 3 and 5 since D' is obtained from a continuous distribution function. Both the North Carolina and Florida case studies were observed to have a maximum contribution to sky cover in the counting interval centered at 1.91 km. The value of D' for the North Carolina data was within this class interval while the value of D' for the Florida data was found to exceed the upper bound of the class interval by only 0.04 km.

In comparing the DMSP oceanic samples to the two previous cases, the first parameter that shows a marked difference is D_m , the maximum

diameter cloud observed. The range of diameters observed in the oceanic case study is at least 1.91 km, or two class intervals, less than the range observed in the continental case studies.

The total number density observed in the DMSP oceanic samples was slightly less than the number densities observed over land. As with the Florida data, the theoretical value of N_T is 33% less than the observed value, indicating a regression equation which predicts too low a number density in the smaller diameter classes. Figure 6 bears this out, showing the regression equation to be deficient in the first two class intervals.

The observed value of S_T for the DMSP oceanic case study showed a 51% decrease from that obtained from the North Carolina data and a 31% decrease in sky cover when compared to the Florida samples. The theoretical value of S_T slightly overestimated the value actually observed, having an error of only 0.5%.

While the slope of the regression equation is observed to be greater for the DMSP oceanic data than for either of the two continental data sets, two important points must be recalled. First, the influence of cloud groups is present in the number density distributions reported in Table 13. The effect of removing these cloud groups will be discussed in the next section of this paper. Second, the regression equations presented in chapter three are computed using mean cloud number densities rather than the individual sample number densities. The validity of such computations will be discussed in section 3.2.3.

The modal diameter for sky cover in the DMSP oceanic case was found to be in the second counting interval, centered at 1.91 km (see Figure 7). The predicted modal diameter, D' , was calculated to be 2.04 km which is in excellent agreement.

The SMS-1 oceanic case study parameters differed from the previous three cases in many ways. The first difference noted was the smallest diameter cloud observed during sampling. In the three DMSP cases, the smallest diameter cloud was limited only by the resolution of the satellite. With the SMS-1 imagery, however, the lower limit seems to be affected more by data quality than by satellite resolution. The SMS-1 data lacked the contrast and definition present in the DMSP imagery. This made detection and measurement of the smaller clouds much more difficult than in the three case studies discussed. The lower limit of observed cloud diameters was placed at 1.1 km, the lower bound of the first counting interval.

The largest cloud diameter observed in the SMS-1 samples was 1.04 km; thus the range of cloud diameters observed was more like the continental samples than the other maritime case.

The total cloud number density, N_T , was observed to be one-fourth to one-third that observed in the other case studies. This is primarily caused by the inability of the analyst to adequately discern the smaller clouds. Due to the exponential decrease in number density with increasing size, total number density is most affected when the smaller class intervals are found to be deficient.

The theoretical cloud number density obtained for the SMS-1 data is identical to the observed number density, indicating a good fit of

the regression line to the data in the smaller diameter counting classes (see Figure 9).

The total sky cover for the SMS-1 case study, observed to be 6.28%, falls in the range described by the other case studies. The theoretical total sky cover agreed quite well with the observed value, having an error of only 1.6%.

The slope of the regression line calculated for the SMS-1 case study is much less than the other three case studies. The decrease in slope is felt to be the result of two separate effects. The first effect, that of inadequately detecting the smallest clouds, has already been discussed. The second reason the slope is decreased lies in the fact that cloud groups were included in the calculation of the regression line. While the effect of group structures can be removed, little can be done concerning the problem of data quality.

Because the DMSP oceanic samples were taken from the western portion of the Atlantic Ocean and the Gulf of Mexico, there might be reason to believe that the samples taken from the eastern part of the Atlantic Ocean, comprising the SMS-1 oceanic case study, might exhibit a change in regression slope due to differing meteorological conditions in the two areas. To investigate this line of reasoning, the ideal test would be to examine the SMS-1 sampling areas using data taken from the DMSP vehicle. Since the data were not available, an alternative test using a single sample of DMSP Block 5D imagery was conducted. Although a single sample will not yield any statistically significant results, some insight can hopefully be gained.

The Block 5D vehicle is the latest satellite in the DMSP inventory, attaining operational status late in the spring of 1977. Because it has been operational for such a short time, not enough data yet exists to select a significant number of samples for a case study.

The sample was selected from vehicle number 12535, orbit number 3829, which had an ascending node time of 1124Z on 8 June 1977. The sampling area was bounded by the equator, 1S, 4E, and 5E. A total of 115 clouds were tabulated within the sampling area, with diameters ranging from 0.6 km to 2.87 km. The slope of the regression line calculated for this sample was 1.3794, which is much greater than any of the case studies reported in Table 13. These results, although not conclusive, would lead one to believe that SMS-1 data quality rather than differing meteorological conditions had caused the change in slope.

3.2.2 Group Structure Analysis

Four types of cloud structures were observed in the analysis of the satellite data. The first type, seen in Figure 11A, represents individual cumulus cells which constituted the vast majority of the clouds tabulated. Figure 11B depicts a cloud group structure in which a fairly large central cell ($D_1 \approx 3$ to 6 km) is joined to one or more very small cells. In most cases the junction point was discernable and the components of such a group structure were tabulated as individual cloud cells.

Group structures in which the component cells could not be discerned were recorded in a slightly different manner. For clouds of

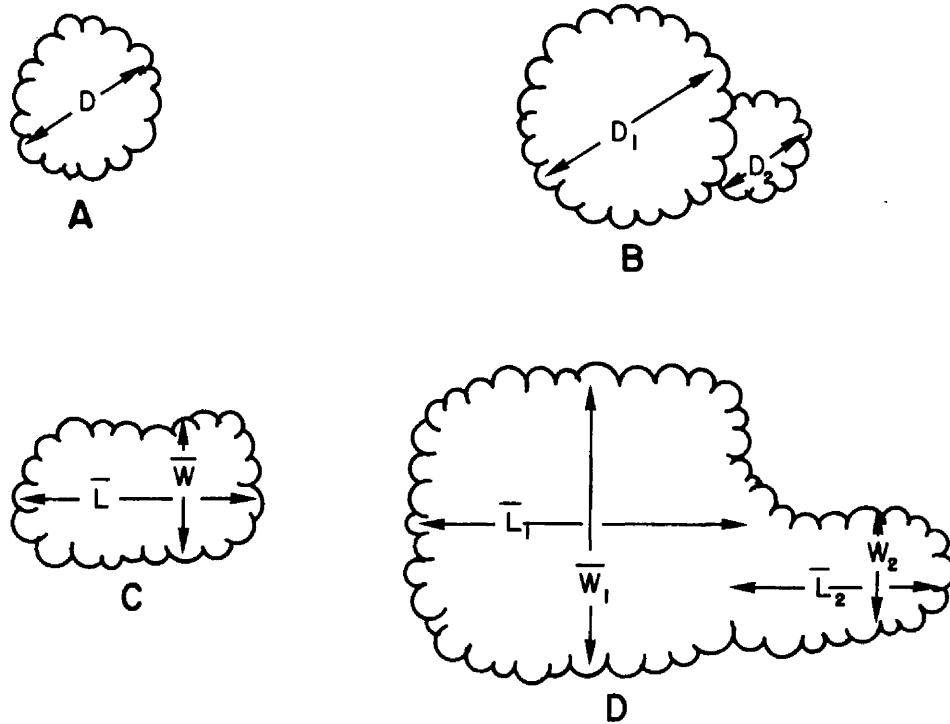


Figure 11. Configurations of Clouds Observed in Sampling.

the types seen in Figures 11C and 11D, the mean lengths and widths were recorded and the cloud base cross-sectional areas were calculated. An equivalent cloud diameter was then computed for each cloud from the relationship $D = 2 \left(\frac{\bar{W}_i \bar{L}_i}{\pi} \right)^{1/2}$. These clouds were then tabulated by their equivalent diameters along with the types of clouds mentioned in the previous paragraph. By keeping a separate record of the cloud group structures, their effect on the number density distribution can be easily removed.

Removal of the cloud groups is required in order to make a relevant comparison with the results of the study made by Plank. Table 14 presents the results of the four case studies after the contributions made by cloud groups are eliminated. The first notable change is the reduction in the range of diameters observed. The maximum cloud diameter observed in the North Carolina, Florida, and SMS-1 oceanic case studies is now approximately 6.7 km instead of values greater than 9.0 km (see Table 13). The maximum cloud diameter observed in the DMSP oceanic case study was reduced by 50%, from 7.63 km to 3.82 km.

The total cloud number density values, both observed and theoretical, are seen to be in excellent agreement among the three DMSP case studies. The SMS-1 case study showed a decrease of 13% in the total number density observed, while the theoretical value of N_T remained constant. Those case studies which exhibited the largest changes in observed total number density also had the largest complement of cloud group structures present in the original analysis. For example, the North Carolina and SMS-1 case studies each had approximately 15% of their size distributions composed of group structures. The Florida

Table 14. Summary of Results, Cloud Groups Excluded.

Case Study	d (km)	D_m (km)	N_T	N_T	S_T	S_T	α (km^{-1})	αD_m	χ	D' (km)
	Observed	Observed	Observed	Theoretical	Observed	Theoretical				
North Carolina	0.6	6.67	29	33	0.0705	0.0713	1.1993	8.00	0.947	1.67
Florida	0.6	6.67	31	31	0.0582	0.0588	1.3054	8.71	0.944	1.54
DMSP Oceanic	0.6	3.82	30	33	0.0493	0.0518	1.4967	5.72	0.857	1.33
SMS-1 Oceanic	1.1	6.67	7	9	0.0368	0.0373	1.0011	6.68	0.860	2.02

Note: The original data from which this summary was compiled can be found in Appendix B.

case study, having only 8% of the distribution contained in cloud groups, showed a smaller change in N_T than the North Carolina or SMS-1 data. No change was seen in the DMSP oceanic case study as it contained only 2% of the distribution in cloud groups.

The same relative decreases seen in the observed total number densities are also reflected in the observed total sky cover values for the four case studies. The theoretical values of S_T obtained for all cases were overestimates of the observed values with errors ranging from 1% to 5%.

The removal of cloud groups primarily affects the number density distribution by eliminating the larger diameter class intervals and reducing the number densities of the intermediate classes. The smaller diameter class intervals are virtually unaffected. The change in slope of the regression line resulting from the elimination of group structures is a measure of these effects. The three DMSP case studies showed an increase in slope which ranged from 32% to 64%. While the SMS-1 data did not produce a slope of the same magnitude as the DMSP samples, the increase in slope was the largest at 67%.

3.2.3 Statistical Analysis

One of the major problems in fitting an exponential model of the form $n = Ke^{-\alpha D}$ to a data set arises from the fact that a solution of the model may never equal zero. The normalized cloud number densities presented in Tables 2 through 11 were often observed to be zero, especially in the larger diameter class intervals. Another problem which arises in the use of an exponential model concerns the

non-linearity of such a model. This problem is easily overcome by a simple logarithmic transformation of the model to the form $\ln n = -\alpha D + b$. In such a form, the model can be analyzed using simple linear regression techniques. Although the model is now easier to analyze, one is still confronted with the initial problem, the inability of the model to treat null observations.

The simplest method of dealing with the problem of class intervals which contain zeroes is to obtain the mean number density of the class interval and use the mean in computing the regression equation. The regression equations presented in sections 3.1.1 through 3.1.4, as well as the values of α seen in Tables 13 and 14, are the results of such a treatment.

Problems arise from such a simplistic solution, however. First, class intervals that have a mean number density of zero cannot be included in the analysis. While this occurrence was found to be the exception rather than the rule, two class intervals from each of the oceanic case studies were excluded from the analysis for this reason (see Tables 8 and 11). The exclusion of entire class intervals raises the question of whether or not the model is adequate in describing the mean number density distribution of cumulus clouds. Unfortunately, by using the mean number density for each class interval, statistical testing of the adequacy of the model is impossible.

In order to test the adequacy of the model, replications are required within the class intervals. These replications are present in the data sets in the form of individual sample observations. The observations of zero number density can be readily included if the

model is modified slightly to take the form $\ln(n+c) = -\alpha D + b$, where c is a small constant added to the observed cloud number density. The value of c chosen for the analysis of the four case studies was 1.0×10^{-3} , which was one order of magnitude smaller than any observed number density. The addition of such a small constant allows adequate representation of the null observations while minimizing the change in the remaining observations. The model was run in this modified form to test the significance of regression and the adequacy of the model. Two regression equations were calculated for each case study to examine the effects of including cloud groups or omitting them from the analysis. At the .01 significance level, the tests for significance of regression yielded positive results in all eight cases (see Appendix A). The results of the tests for adequacy of the model were almost as encouraging, with seven of the eight regression lines exhibiting no significant lack of fit at the .01 significance level.

The single case which showed significant lack of fit was found to be the DMSP oceanic case study when cloud groups were included in the analysis (see Table 7A, Appendix A). The lack of fit in the model can be explained if one considers the original data, shown in Table 8. The largest diameter class interval is composed of a single cloud group which is separated from the remaining classes of the distribution by two class intervals in which no clouds were observed. By including this one cloud group in the regression analysis, the model attempts to fit the single cloud group and the seventeen null observations required to represent it properly. This attempt is made at the expense of an adequate fit to the 572 clouds which make up the remaining class

intervals. If the single cloud group is treated as an outlier and is removed from the analysis, the model is then adequate in describing the remaining points with no significant lack of fit evident at the .01 significance level (see Table 9A, Appendix A).

3.2.4 Comparison to Previous Research

Before any comparison to previous investigators' results could be made, a typical sample had to be chosen for each case study area (see Figures 12 through 15). The selection procedure outlined in Appendix B was followed to ensure that the sample was representative of the area in terms of the mean number densities and range of diameter classes observed. The selected samples have been summarized in Table 15 along with typical samples reported by previous researchers. The two samples attributed to Plank are taken from his category of "average sky cover". The results of Blackmer and Serebreny are taken from the paper by Plank (1969). All results in the table which are attributed to other investigators have been converted to units of measure used in this research effort.

The first difference in results that is readily apparent is in the diameter of the smallest cloud observed in the samples. Although there is approximately an order of magnitude difference between the current results and those of previous research, it should be recalled that the previous sampling was done from aircraft reconnaissance photographs. The resolution of the photographs used by Plank was on the order of 15 meters, while the data used by Blackmer and Serebreny had a resolution of approximately 150 meters.

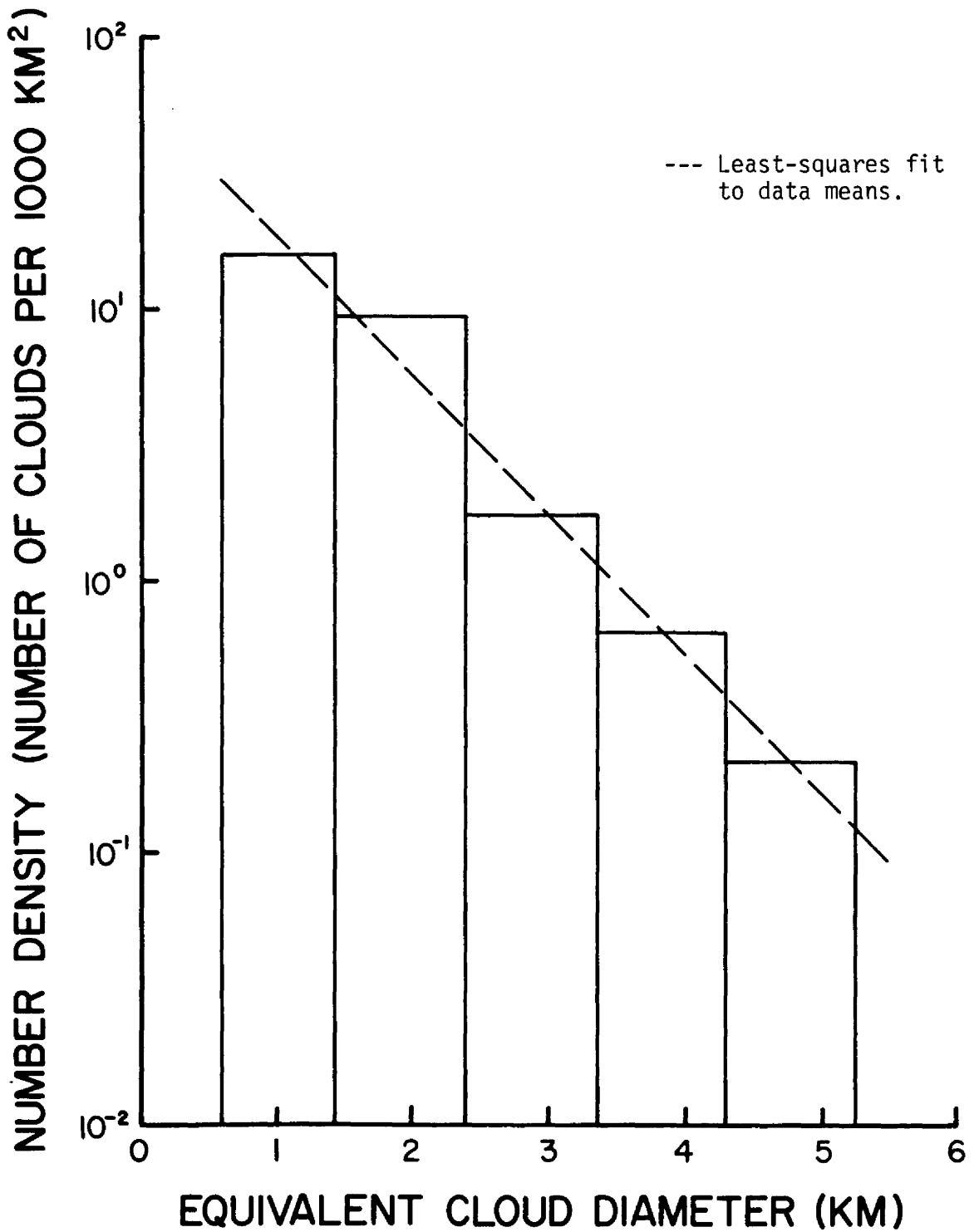


Figure 12. Typical North Carolina Sample, 2 June 1973.

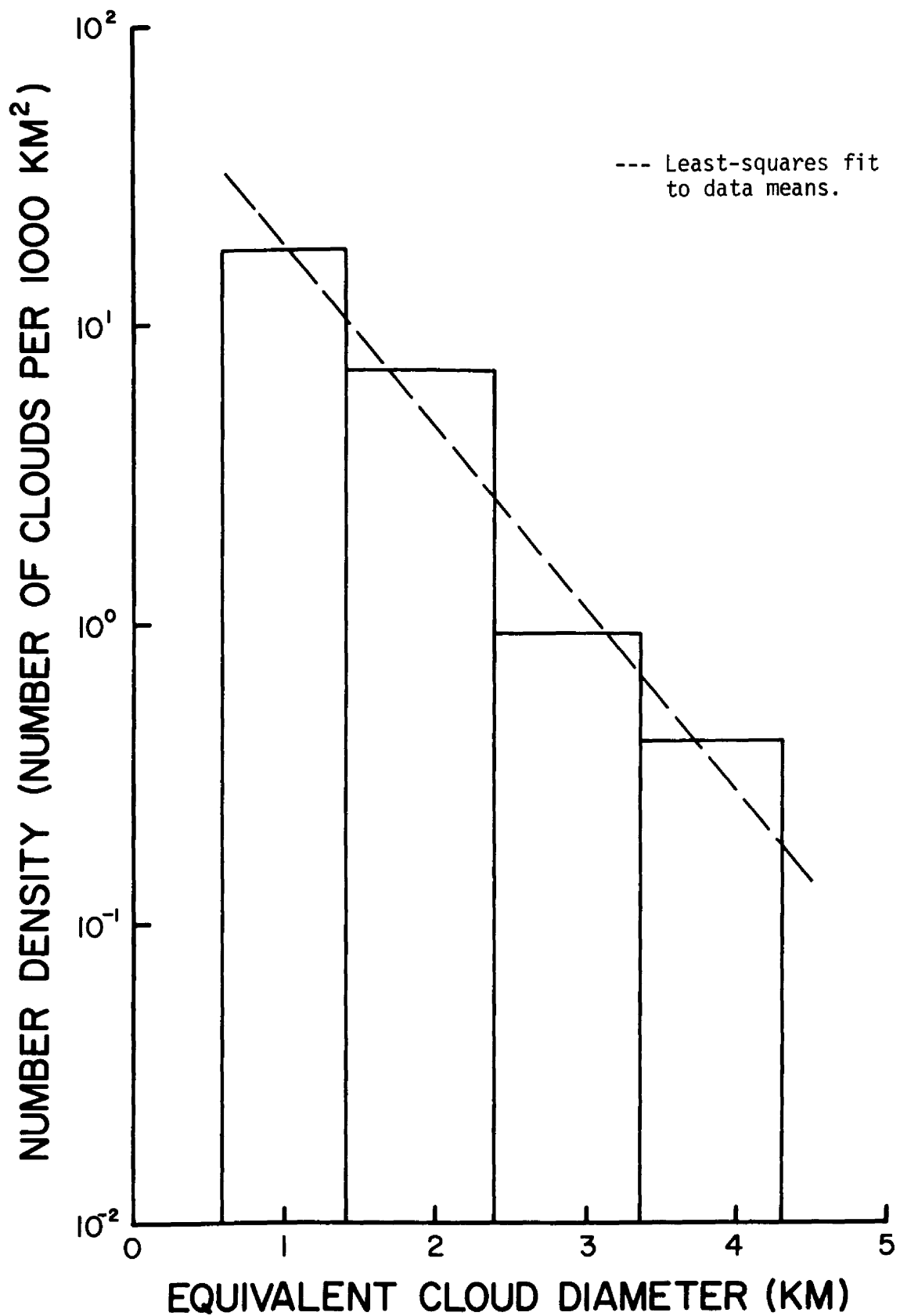


Figure 13. Typical Florida Sample, 14 June 1973.

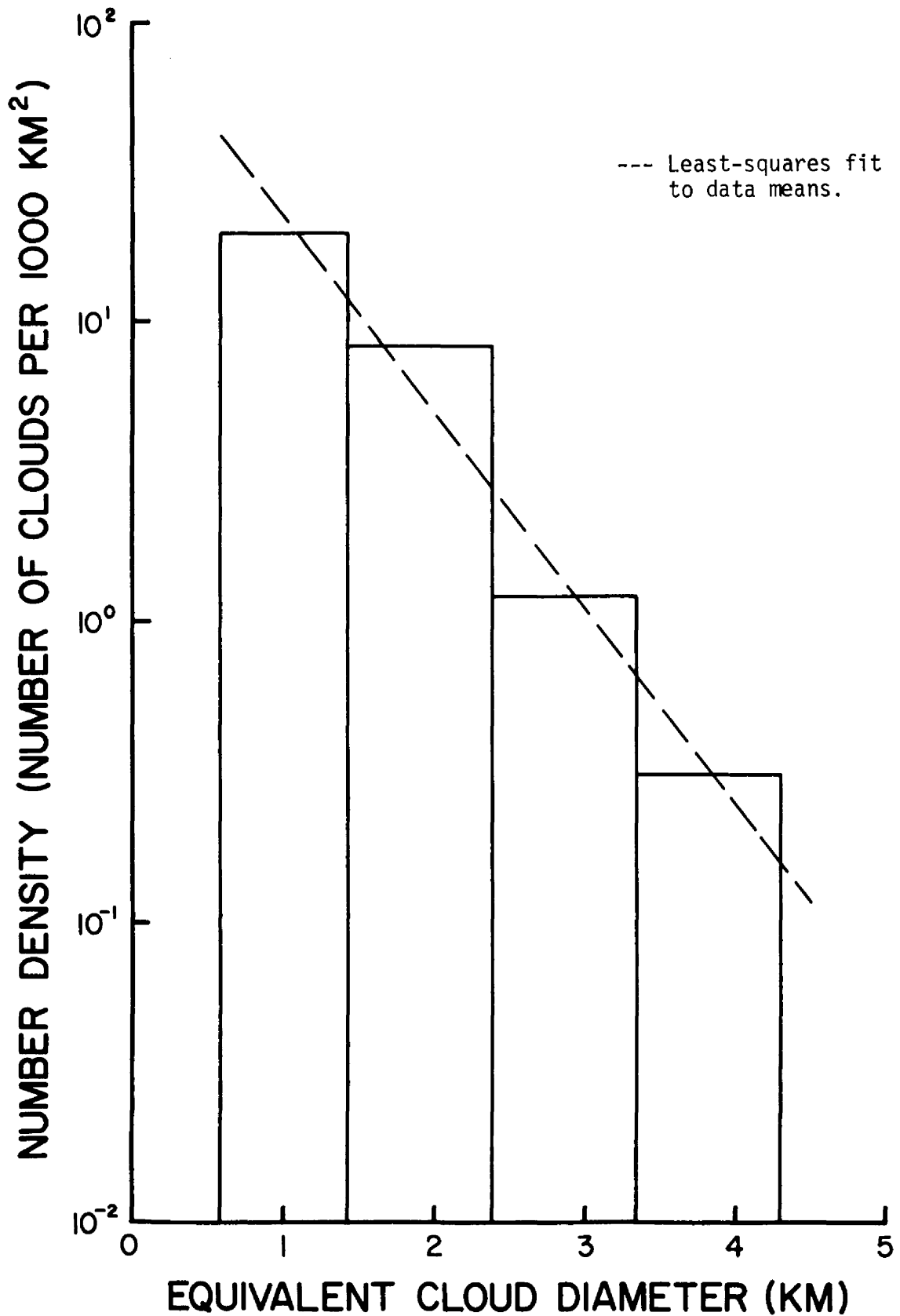


Figure 14. Typical DMSP Oceanic Sample, 29 August 1973.

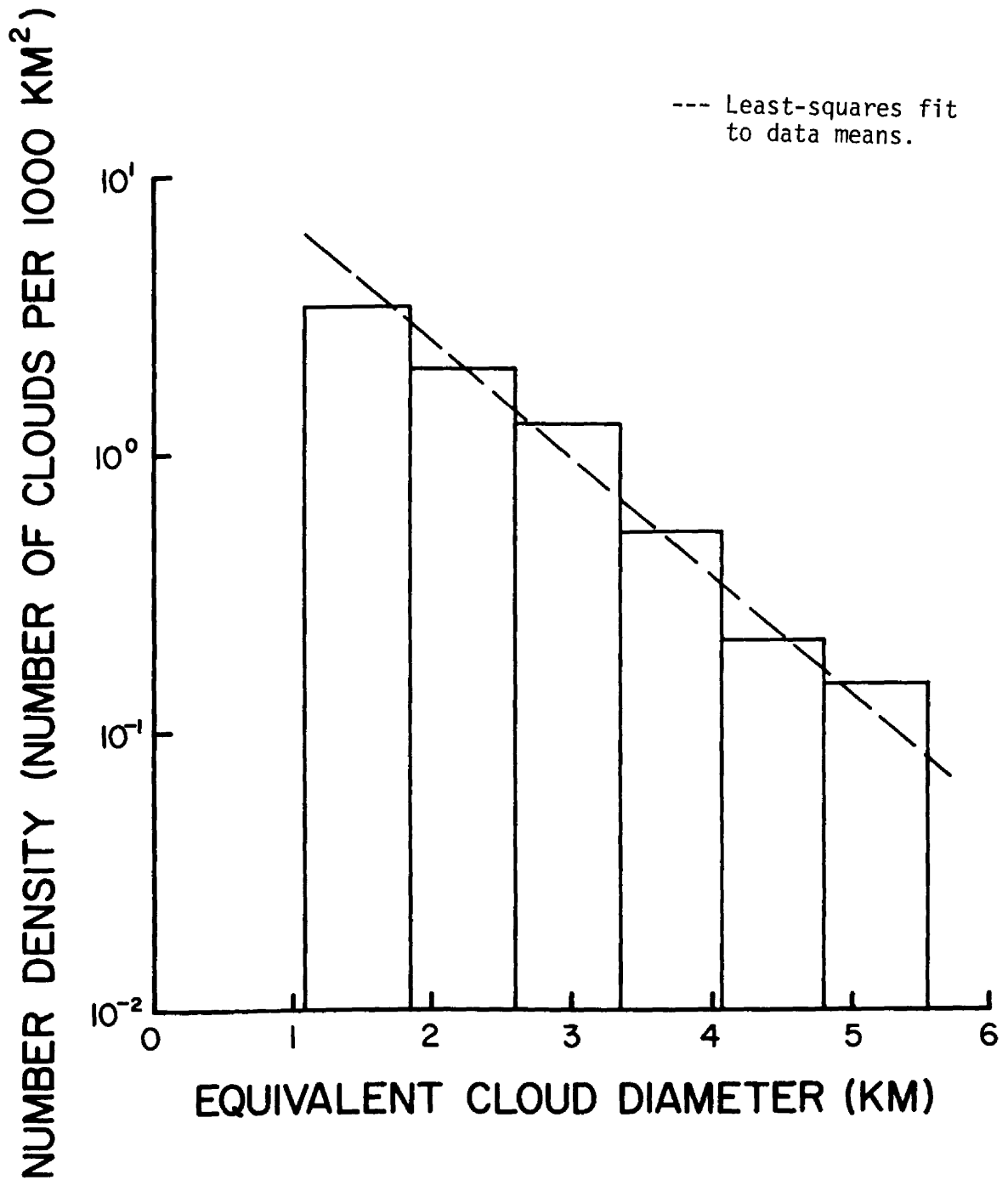


Figure 15. Typical SMS-1 Oceanic Sample, Day 247, 1974.

Table 15. Summary of Parameters for Typical Cumulus Samples.

Investigator	Area	Sampling Time (Local)	d (km) Obs.	D _m (km) Obs.	N _T Obs.	N _T Th.	S _T Obs.	α (km ⁻¹)	αD _m	χ	(km)
Gifford	N. Carolina	1200	0.6	4.78	28	30	0.061	1.17	5.59	0.882	1.70
Gifford	Florida	1200	0.6	3.82	26	27	0.043	1.39	5.31	0.846	1.43
Gifford	DMSP Oceanic	1200	0.6	3.82	30	33	0.049	1.51	5.77	0.860	1.31
Gifford	SMS-1 Oceanic	1100	1.1	5.19	8	9	0.034	0.97	5.03	0.780	2.07
Plank	Florida	1100-1200	0.022	2.78	4742	1466	0.309	2.71	7.53	0.921	0.74
Plank	Florida	1200-1300	0.022	3.41	4400	990	0.349	2.05	6.99	0.897	0.98
Blackmer & Serebreny	Miss., Tex., N. Mex., Cal.	1210-1510	0.161*	3.54	540	718	0.3*	2.32	8.21	0.984	0.87
Blackmer & Serebreny	Fla., Miss., Tex.	1220-1530	0.161*	6.61	286	219	0.3*	1.17	7.73	0.983	1.70
Blackmer & Serebreny	Fla., Ala., N. Mex., AZ.	1140-1530	0.161*	11.40	216	82	0.3*	0.69	7.87	0.984	2.93

Note: * = Assumed values.

The maximum diameter clouds observed in the current samples are in good agreement with those reported by Plank. Although the values of D_m for the four current cases fall within the range described by Blackmer and Serebreny, it was unclear whether or not cloud groups were removed from their distributions. It would therefore be advisable to compare the results of Blackmer and Serebreny with the summary of results shown in Table 13 as well as those shown at the top of Table 15.

The total cloud number densities, N_T , are seen to differ from Plank's results by approximately three orders of magnitude. Again, this disparity is caused by the difference in system resolutions. For instance, of the 4742 clouds per 1000 km² reported by Plank, over 4375 clouds per 1000 km² were tabulated in the range from 0.022 km to 0.167 km. Another 260 to 290 clouds per 1000 km² were found in the range from 0.167 km to 0.648 km. Therefore, what initially seems to be a large discrepancy in results is in reality a close agreement if the effects of resolution are eliminated. Apparent disagreement with the results of Blackmer and Serebreny can also be dismissed with the same argument.

There is good agreement between observed and theoretical values of N_T among the four samples representing the current case studies. Plank's results show great deficits in the theoretical values of N_T for both samples. This deficit is the result of not including the two smallest class intervals (diameters < 0.167 km) in the calculation of a regression equation. These two class intervals were omitted due to uncertainty in the accuracy of the data. As a result, the regression

line cannot possibly account for the large number of clouds contained in the smallest classes. Similar disagreements are seen in the results of Blackmer and Serebreny, although not as large an error is noted. These disagreements also seem to be caused by a poor fit of the regression line in the smallest class intervals.

The total sky cover is seen to range from approximately 3% to 6% for the cases under current investigation while previous research yields results approximately five times as great. As before, the disagreement is linked to the differences in resolution between the two types of data. Recalling the sky cover relationship $s = \frac{\pi D_i^2 n_i}{4}$, and assuming \bar{n}_i is approximately 1460 clouds per 1000 km² for the diameter interval from 0.019 km to 0.93 km, one obtains a sky cover contribution of 24.5% for this interval. Therefore, the contributions to total sky cover which can occur below the resolution of the satellite data are seen to make up a substantial portion of the differences observed. The total sky cover was not reported by Blackmer and Serebreny; Plank assumed the 35% value that appears in the table.

The values of α calculated for the current samples are seen to fall within the range reported by Blackmer and Serebreny, while Plank observed regression slopes approximately twice as large. However, Plank points out that the intermediate classes are slightly over-estimated by the regression lines describing some of his samples as well as those of Blackmer and Serebreny. Their intermediate classes, with cloud diameters ranging from 0.65 km to approximately 1.67 km, correspond to the smallest class intervals of the present study. If the regression equations had been calculated with the lower bound set

at approximately 0.65 km, the agreement between the resulting slopes would be somewhat improved. Also shown by the satellite derived distributions was the tendency for α to decrease as D_m increased, a tendency which was evidenced in both photographic studies.

The values of αD_m and χ are seen to agree quite well with the exception of the Blackmer and Serebreny results. The inflated results are quite possibly caused by the inclusion of cloud groups in their distributions. The values of αD_m and χ shown in Table 13, which summarizes the mean distributions including group structures, are quite similar to those reported by Blackmer and Serebreny.

For the four satellite samples, the predicted modal diameter for sky cover, D' , was in fair agreement with the values observed, considering the large class intervals used in this study. The three DMSP samples were all observed to have a maximum contribution to S_T in the second counting interval which has 1.44 km and 2.41 km as its lower and upper bounds. The value of D' is seen to lie within this class interval in the North Carolina distribution, while for the remaining DMSP samples the predicted value falls just below the lower bound of the correct class. The SMS-1 sample was observed to make its largest contribution to total sky cover in the third class interval, bounded by 2.59 km and 3.33 km. The predicted modal diameter falls near the middle of the next smaller class interval.

4.0 CONCLUSIONS

The research reported in this paper was conducted to determine the applicability of satellite data in determining the size distributions of fields of small-scale cumulus. The techniques used in this investigation are unique in that they allow the analyst to fully utilize the satellite imagery, being limited only by the resolution of the data. With the improved resolution of the newer generation satellite vehicles, such as the Block 5D platform of the Defense Meteorological Satellite Program, future research of this type will yield even more reliable results.

The mean cloud number densities for all four case studies were seen to decrease exponentially with increasing cloud diameter, confirming the findings of previous investigators. Of the twenty-four individual samples studied, twenty-one followed this tendency while three of the SMS-1 samples were seen to be deficient in the smallest class interval. The reason given for the deficiencies was the poorer quality of the SMS-1 imagery compared to that of the DMSP data. The effect of poor data quality was felt in the mean cloud number density distribution obtained for the SMS-1 data, resulting in a coefficient of exponential decrease in cloud number density, α , which was substantially lower than those values calculated for the three DMSP case studies. Future research should include concurrent sampling in an attempt to test the conclusion that SMS-1 imagery lacks the resolution required by this type of study.

It was hoped that by choosing several samples from varying locations, differences in distribution parameters would become evident. This was not found when typical samples from the case studies were compared in Table 15. In fact, the distribution parameters of the three DMSP samples were found to be remarkably similar. There was a slight increase in the slope of the regression equation obtained for the oceanic sample when compared to the two continental samples. The increase in slope was also noticed when comparing parameters derived from the mean number density distributions of entire case studies. When the slopes of the typical North Carolina and DMSP oceanic samples are compared, a statistically significant difference can be shown to exist at the .05 significance level (see Appendix C). The acceptance of such statistical results must be made with reservation, however, since so few degrees of freedom are contained in the data.

One method of increasing the number of degrees of freedom in future experiments of this nature would be to enlarge the satellite imagery photographically. Enlargement would result in a larger number of class intervals within an observed diameter range. This method of analysis would probably reduce measurement error in the smaller diameter classes while simultaneously decreasing the amount of analysis time required for each sample.

Another method of increasing the number of degrees of freedom would be to use an optical digitizing system to automate the sampling procedure. The digitizing equipment currently in use at Colorado State University has several features which could be extremely helpful in future research. First, the data can be enlarged to a scale which

would facilitate analysis, with benefits similar to those of photographic enlargement mentioned previously. Also, the equipment can be operated in the low-enhancement mode which would give greater contrast between the lower albedo cumulus clouds and the surface of the earth. In addition to size distributions, optical digitization would yield information concerning the relative albedos of the clouds within any given sample.

Finally, in order to increase the number of degrees of freedom inherent in the data more samples could be included in each case study. The additional samples would result in much more conclusive statistical results, especially when testing for lack of fit of the exponential model. Also, a greater number of samples would allow for categorization of the results into classes which could subsequently be related to varying synoptic scale and mesoscale atmospheric conditions.

REFERENCES

- Blackmer, R. H. and S. M. Serebreny, 1962: Dimensions and Distributions of Cumulus Clouds as Shown by U-2 Photographs. Unpublished Manuscript, Stanford Research Institute, AFCRL Rept. No. 62-609.
- Dickinson, Lee G., S. Edward Boselly III, and Walter S. Burgmann, 1974: Defense Meteorological Satellite Program (DMSP) User's Guide. Air Weather Service Tech. Rept. 74-250, USGPO, December.
- Gray, William M., 1973: Cumulus Convection and Larger Scale Circulations I. Broadscale and Mesoscale Considerations. Mon. Wea. Rev., 101, 12.
- Lopez, Raul Erlando, 1973: Cumulus Convection and Larger Scale Circulations II. Cumulus and Mesoscale Interactions. Mon. Wea. Rev., 101, 12.
- Lopez, Raul Erlando, 1976: Radar Characteristics of the Cloud Populations of Tropical Disturbances in the Northwest Atlantic. Mon. Wea. Rev., 104, 3.
- McKee, Thomas and Stephen K. Cox, 1974: Scattering of Visible Radiation by Finite Clouds. J. Atmos. Sci., 31, 1885.
- McKee, Thomas B. and Stephen K. Cox, 1976: Simulated Radiance Patterns for Finite Cubic Clouds. J. Atmos. Sci., 33, 2014.
- Plank, Vernon G., 1969: The Size Distribution of Cumulus Clouds in Representative Florida Populations. J. Appl. Meteor., 8, 1.
- Reynolds, David W. and Thomas H. Vonder Haar, 1975: Satellite Support to the HIPLEX Activities for 1974. Final Report to Bureau of Reclamation, Contract No. 14-06-D-7630.
- Smithsonian Meteorological Tables, prepared by Robert J. List, 6th Revised Edition, 1971. Smithsonian Institution Press, Washington, D.C.
- Snedecor, George W. and William G. Cochran, 1971: Statistical Methods, Sixth Edition. Iowa State University Press, Ames, Iowa.
- Stodt, Richard W. and Lewis O. Grant, 1976: Satellite Cloud Climatology of Summertime Cumulus Research Areas. Preprints of the International Conference on Cloud Physics, WMO, Boulder, Colorado, July.
- Stoldt, Norman W. and Peter J. Havanac, 1973: Compendium of Meteorological Satellites and Instrumentation. National Space Science Data Center, Greenbelt, Maryland, July.

APPENDIX A.

STATISTICAL RESULTS

In order to test the significance of regression and the adequacy of the linearized model, analysis of variance was performed on the data gathered for each case study. The resulting AOV tables are presented as Tables 1A through 9A. As mentioned in chapter 3.2.3, a small constant (.001) was added to the data in order to adequately represent the data points recorded as zeroes.

Two statistical tests can be performed on the information presented in the AOV tables. The first test examines the significance of the regression and uses the null hypothesis $H_0 : \hat{\beta}_1 = 0$, where $\hat{\beta}_1$ is the estimated slope of the regression line. In testing the null hypothesis, the F ratio $F_{\text{calc}} = \frac{MS_{\text{regression}}}{MS_{\text{residual}}}$ is compared to the tabled value of F at a given significance level. The values shown in the AOV tables in the column labeled $F_{.01}$ are the values which correspond to the .01 significance level for the indicated number of degrees of freedom. Since $F_{\text{calc}} > F_{.01}$ in all cases, the null hypothesis must be rejected, indicating that the regression slope is significantly different from zero in all cases.

The second test examines the null hypothesis that the model is adequate in describing the data points. In this test, the value of F_{calc} is the ratio $\frac{MS_{\text{Lack of fit}}}{MS_{\text{Pure error}}}$. If the value of $F_{\text{calc}} > F_{.01}$, then the null hypothesis must be rejected, indicating an inadequate model. The null hypothesis was rejected only once (see Table 7A).

The inflated mean square for lack of fit was assumed to be caused by an outlier in the data. Removal of the suspected outlier reduced the calculated F value to the extent that the null hypothesis could not be rejected (see Table 9A).

Table 1A. AOV Table for North Carolina Case Study.

Cloud group structures are included in the number density distribution. Regression equation: $\ln(n + .001) = -1.2105 D + 4.4198$. Correlation coefficient = -0.8857.

Source	SS	DF	MS	F _{calc}	F _{.01}
Regression	438.9318	1	438.9318	203.9362	7.22*
Residual	103.3123	48	2.1523		
Pure Error	85.5352	40	2.1384		
Lack of Fit	17.7771	8	2.2221	1.0391	2.99
Total _{corrected}	542.2441	49			
* Interpolated value					

Table 2A. AOV Table for North Carolina Case Study.

Cloud group structures have been eliminated from the number density distribution. Regression equation: $\ln(n + .001) = -1.6273 D + 4.9394$. Correlation coefficient = -0.8570.

Source	SS	DF	MS	F _{calc}	F _{.01}
Regression	276.8677	1	276.8677	111.8883	7.49*
Residual	81.6262	33	2.4745		
Pure Error	78.6575	28	2.8092		
Lack of Fit	2.9687	5	0.5937	0.2114	3.75
Total _{corrected}	358.4939	34			
* Interpolated value					

Table 3A. AOV Table for Florida Case Study.

Cloud group structures are included in the number density distribution. Regression equation: $\ln(n + .001) = -1.0305 D + 2.9304$. Correlation coefficient = -0.8028.

Source	SS	DF	MS	F _{calc}	F _{.01}
Regression	438.9318	1	502.7806	128.1227	7.06*
Residual	251.1496	64	3.9242		
Pure Error	194.1353	55	3.5297		
Lack of Fit	57.0143	9	6.3349	1.7947	2.76*
Total _{corrected}	753.9302	65			
* Interpolated values					

Table 4A. AOV Table for Florida Case Study.

Cloud group structures have been eliminated from the number density distribution. Regression equation: $\ln(n + .001) = -1.7525 D + 4.6846$. Correlation coefficient = -0.8486.

Source	SS	DF	MS	F _{calc}	F _{.01}
Regression	377.9851	1	377.9851	117.9950	7.31
Residual	128.1377	40	3.2034		
Pure Error	114.9073	35	3.2881		
Lack of Fit	13.2304	5	2.6461	0.8060	3.60*
Total _{corrected}	506.1228	41			
* Interpolated value					

Table 5A. AOV Table for SMS-1 Oceanic Case Study.

Cloud group structures are included in the number density distribution. Regression equation: $\ln(n + .001) = -0.9694 D + 2.4598$. Correlation coefficient = -0.8280.

Source	SS	DF	MS	F _{calc}	F _{.01}
Regression	506.2887	1	506.2887	202.9374	6.96*
Residual	222.0374	89	2.4948		
Pure Error	166.8017	78	2.1385		
Lack of Fit	55.2357	11	5.0214	2.3481	2.49*
Total _{corrected}	728.3261	90			
* Interpolated values					

Table 6A. AOV Table for SMS-1 Oceanic Case Study.

Cloud group structures have been eliminated from the number density distribution. Regression equation: $\ln(n + .001) = -1.4799 D + 3.9906$. Correlation coefficient = -0.8409.

Source	SS	DF	MS	F _{calc}	F _{.01}
Regression	270.6996	1	270.6996	148.4994	7.15*
Residual	98.4352	54	1.8229		
Pure Error	78.6096	48	1.6377		
Lack of Fit	19.8256	6	3.3043	2.0176	3.22*
Total _{corrected}	369.1348	55			
* Interpolated values					

Table 7A. AOV Table for DMSP Oceanic Case Study.

Cloud group structures are included in the number density distribution. Regression equation: $\ln(n + .001) = -1.6724 D + 4.4865$. Correlation coefficient = -0.8765.

Source	SS	DF	MS	F _{calc}	F _{.01}
Regression	497.5262	1	497.5262	171.2655	7.24*
Residual	133.6296	46	2.9050		
Pure Error	61.1405	40	1.5285		
Lack of Fit	72.4891	6	12.0815	7.9041	3.29
Total _{corrected}	631.1558	47			

* Interpolated value

Table 8A. AOV Table for DMSP Oceanic Case Study.

Cloud group structures have been eliminated from the number density distribution. Regression equation: $\ln(n + .001) = -2.0149 D + 5.4038$. Correlation coefficient = -0.8081.

Source	SS	DF	MS	F _{calc}	F _{.01}
Regression	98.7276	1	98.7276	53.0565	7.95
Residual	40.9368	22	1.8608		
Pure Error	35.9758	20	1.7988		
Lack of Fit	4.9610	2	2.4805	1.3790	5.85
Total _{corrected}	139.6644	23			

Table 9A. AOV Table for DMSP Oceanic Case Study.

Cloud group structures are included in the number density distribution, but the outlier (4.12 NM class) has been removed from the analysis. Regression equation: $\ln(n + .001) = -2.2225 D + 6.0080$. Correlation coefficient = -0.8573.

Source	SS	DF	MS	F _{calc}	F _{.01}
Regression	231.3603	1	231.3603	112.8862	7.64
Residual	57.3871	28	2.0495		
Pure Error	43.3911	25	1.7356		
Lack of Fit	13.9960	3	4.6653	2.6879	4.68
Total _{corrected}	288.7474	29			

APPENDIX B.

SELECTION OF TYPICAL SAMPLES

In order to select a typical sample from each case study area, the normalized cloud number densities (excluding cloud groups) were first computed for each sample. A mean cloud number density was then found for each class interval of a given case study. The resulting tabulation for each case study area can be seen in Tables 1B through 4B. Finally, all samples within a given case study were compared to the mean number densities and a selection of the most representative sample was made. The selected sample from each case study is indicated by an asterisk in the tables. A regression line was then computed for each of the typical samples.

Table 1B. Normalized Cloud Number Densities for North Carolina, Excluding Cloud Groups.

Date	Equivalent Cloud Diameter, km						
	0.96	1.91	2.87	3.82	4.78	5.72	6.69
*2 June 73	15.7	9.37	1.74	0.654	0.219	0	0
5 June 73	12.7	10.4	2.25	1.31	0.187	0.187	0
10 July 73	13.8	9.93	3.83	1.78	0.467	0.280	0.093
20 July 73	21.2	11.6	2.50	0.788	0.131	0	0
21 July 73	16.1	6.77	0.876	0	0	0	0
Mean	15.9	9.61	2.24	0.905	0.201	0.093	0.018

* Regression Equation for 2 June 73: $\ln n = -1.1737 D + 4.0865$.

Table 2B. Normalized Cloud Number Densities for Florida, Excluding Cloud Groups.

Date	Equivalent Cloud Diameter, km						
	0.96	1.91	2.87	3.82	4.78	5.72	6.69
4 June 73	32.9	13.3	2.79	1.71	0.181	0	0
*14 June 73	17.7	6.89	0.926	0.412	0	0	0
9 Aug. 73	17.3	9.29	0.400	0.099	0	0	0
10 Aug. 73	12.4	5.58	1.75	0.438	0.108	0	0
20 Aug. 73	17.3	3.74	0	0	0	0	0
30 Aug. 73	24.6	12.4	2.51	0.894	0.269	0.269	0.091
Mean	20.3	8.53	1.40	0.593	0.093	0.044	0.015

* Regression Equation for 14 June 73: $\ln n = -1.3933 D + 4.2901$.

Table 3B. Normalized Cloud Number Densities for DMSP Oceanic Data, Excluding Cloud Groups.

Date	Equivalent Cloud Diameter, km			
	0.96	1.91	2.87	3.82
16 July 73	15.6	7.07	0.710	0
17 July 73	22.5	3.47	0.864	0
18 July 73	27.0	11.1	2.10	0.500
30 July 73	20.0	10.6	1.95	0.277
20 Aug. 73	16.9	4.09	2.34	0.584
*29 Aug. 73	19.7	8.29	1.23	0.307
Mean	20.3	7.45	1.53	0.295

* Regression Equation for 29 Aug. 73: $\ln n = -1.5090 D + 4.6369$.

Table 4B. Normalized Cloud Number Densities for SMS-1
Oceanic Data, Excluding Cloud Groups.

Julian Date	Equivalent Cloud Diameter, km							
	1.5	2.2	3.0	3.7	4.4	5.2	5.9	6.7
228	1.88	2.24	1.06	0.353	0.470	0.117	0	0
229-1	2.33	1.52	0.607	0.102	0.102	0	0	0
229-2	3.04	1.61	0.891	0.091	0.091	0	0	0
238	1.44	1.64	1.44	0.616	1.02	0.204	0	0
239	4.89	3.11	2.05	1.07	0.534	0	0.088	0.088
244	0.602	1.20	1.20	0.841	0.721	0.239	0.359	0
*247	3.39	2.01	1.27	0.531	0.213	0.105	0	0
Mean	2.51	1.90	1.22	0.514	0.450	0.096	0.064	0.012

* Regression Equation for sample 247: $\ln n = -0.9668 D + 2.8436$.

APPENDIX C.

COMPARISON OF REGRESSION SLOPES

The method used for comparing the slopes of two regression equations is explained by Snedecor and Cochran (1971). The two samples being tested here are the samples marked by asterisks in Tables 1B and 3B of Appendix B. The calculations required to make the comparison are shown in the following table:

Table 1C. Comparison of Regression Slopes.

Within Sample	df	Σx^2	Σxy	Σy^2	Reg. Coef.	df	Residual SS	MS
N. Carolina	4	2.6523	-5.7722	12.7832	-2.1763	3	0.2212	0.0737
DMSP Oceanic	3	1.3210	-3.7291	10.5512	-2.8229	2	0.0242	0.0121
						5	0.2454	0.0491
Pooled, W	7	3.9733	-9.5013	23.3344	-2.3913	6	0.6141	0.1024
						1	0.3687	0.3687

To test for a significant difference in slope, the F-test is used. The value of F_{calc} used in this test is the ratio of the mean square residual for a pooled slope, shown on line 5 of the table, divided by the mean square residual obtained when the individual slopes are used, seen on line 3 of the table. The null hypothesis in the test can be expressed as $H_0 : \hat{\beta}_{11} = \hat{\beta}_{12}$, or that the estimated slopes of the two

regression lines are equal. The calculations in the table yield a value of $F_{\text{calc}} = \frac{0.3687}{0.0491} = 7.51$. The F corresponding to 1 and 5 degrees of freedom at the .05 level is 6.61. Since the value of $F_{\text{calc}} > F_{1,5,.05}$ the null hypothesis must be rejected, indicating a significant difference in slope at the .05 significance level.

BIBLIOGRAPHIC DATA SHEET		1. Report No. ATS Paper No. 280	2.	3. Recipient's Accession No.
4. Title and Subtitle Characteristic Size Spectra of Cumulus Fields Observed From Satellites			5. Report Date November 1977	
7. Author(s) Malcolm D. Gifford and Thomas B. McKee			8. Performing Organization Rept. No. 280	
9. Performing Organization Name and Address Dept. of Atmospheric Science Colorado State University Fort Collins, Colorado 80523			10. Project/Task/Work Unit No.	
			11. Contract/Grant No. OCD 75-13924 ATM 76-80568	
12. Sponsoring Organization Name and Address National Science Foundation United States Air Force			13. Type of Report & Period Covered	
			14.	
15. Supplementary Notes				
16. Abstracts <p>A technique is presented which allows the investigator to monitor size distributions of small scale cumulus fields using satellite data. The limitations of the technique are shown to be the resolution and quality of the satellite imagery.</p> <p>Twenty-four samples of small cumulus are studied using DMSP and SMS-1 satellite imagery. A total of eleven DMSP samples are examined from North Carolina and Florida. These samples are compared to six DMSP samples and seven SMS-1 samples drawn from cumulus fields observed over the subtropical and tropical Atlantic Ocean. Comparisons are based on parameters derived from the least-squares solutions of a linearized first order exponential model.</p> <p>An exponential decrease in cloud number density with increasing cloud diameter is exhibited in both the mean cloud number density distributions of the case studies and the cloud number density distributions of selected typical cumulus samples. The poorer data quality of the SMS-1 imagery is seen to cause deviations from the exponential model in approximately 40% of the samples.</p>				
17. Key Words and Document Analysis. 17a. Descriptors <p>Clouds Satellite Radiation</p>				
17b. Identifiers/Open-Ended Terms				
17c. COSATI Field/Group				
18. Availability Statement			19. Security Class (This Report) UNCLASSIFIED	21. No. of Pages 79
			20. Security Class (This Page) UNCLASSIFIED	22. Price